INVESTIGATING THE INFLUENCE OF TEMPERATURE ON KAOLINITE-BASE SYNTHESIS OF ZEOLITE AND UREASE IMMOBILIZATION FOR POTENTIAL FABRICATION OF ELECTROCHEMICAL UREA BIOSENSOR

BY

DAVID EBO ANDERSON

(10552666)

A THESIS SUBMITTED TO THE SCHOOL OF GRADUATE STUDIES, UNIVERSITY OF GHANA, LEGON, IN PARTIAL FULFILMENT OF THE REQUIREMENT FOR THE AWARD OF DEGREE OF MASTER OF PHILOSOPHY (MPhil) IN BIOMEDICAL ENGINEERING

DEPARTMENT OF BIOMEDICAL ENGINEERING

COLLEGE OF BASIC AND APPLIED SCIENCES

UNIVERSITY OF GHANA

MAY, 2018

DECLARATION

I, **DAVID EBO ANDERSON**, do hereby declare that I have duly cited references used in this work, the entire work presented in this thesis, titled "**Investigating the influence of Temperature on Kaolinite-Base Synthesis of Zeolite and Urease Immobilization for Potential Fabrication of Electrochemical Urea Biosensor**" was exclusively done by me, and that, this thesis has never been presented either in part or in whole for any degree in this University or elsewhere.

…… ……

David Ebo Anderson Date

(Student)

…… ……

Elvis K. Tiburu (PhD) Date

(Supervisor)

ABSTRACT

Temperature-dependent zeolite synthesis revealed unique surface morphology, surface area and pore size that influence morphology of zeolite synthesised from kaolin in the immobilization of urease on gold electrode support for biosensor fabrication. XRD characterization identified Zeolite X (Na) at all crystallization temperatures tested. However, Nitrogen adsorption and desorption results showed pore size and pore volume of Zeolite X (Na) 60 °C, Zeolite X (Na) 70 °C and Zeolite X (Na) 90 °C range from 1.92 nm – 2.45 nm and 0.012 cm^3/g – 0.061 cm^3/g respectively, with no significant differences. The specific surface area of Zeolite X (Na) at 60, 70 and 90 °C was 64 m^2/g, 67 m^2/g, and 113 m^2/g respectively. The pore size, specific surface area and pore volumes of Zeolite X (Na) 80 °C and Zeolite X (Na) 100 °C were dramatically increased to 4.21 nm, 295 m^2/g, 0.762 cm^3/g and 4.92 nm, 389 m^2/g, 0.837 cm^3/g in that order. The analytical performance of the embedded urease in Zeolite X (Na) was also investigated using cyclic voltammetry measurements and the results showed distinct cathodic and anodic peaks by Zeolite X (Na) 80 °C and Zeolite X (Na) 100 °C. The molar conductance of the modified zeolite biosensors was measured as a function of urea concentration and gave an average exponential decay regression fit of 0.98. The findings in this study suggest crystallization temperature is a critical parameter for electrochemical analysis of zeolites synthesized from natural sources for various biomedical applications.

DEDICATION

The Almighty God and my family, especially my wife and family gave me encouragement for this work. I wholeheartedly dedicate this work to them.

ACKNOWLEDGEMENT

I am grateful to Almighty God for my life and the strength he imbibed in me in accomplishing this work. I also wish to express my profound gratitude to my supervisor, Dr. Elvis Tiburu, for his mentoring and encouragement during the execution of this thesis. I extend my profound appreciation to all the Lecturers and staff of the Department of Biomedical Engineering for the knowledge and support given to me. My earnest indebtedness goes to the following individuals Srinivasan Shankar, Francis Krampa, Heidimarie N. A. Fleischer and all the staff of WACCBIP (Biochemistry and Biomedical Engineering Department, University of Ghana) for their enormous contribution towards the successful completion of this work.

TABLE OF CONTENTS

LIST OF FIGURES

LIST OF TABLES

LIST OF ABBREVIATIONS

Brunner Emmett Teller……BET

Carbon nanotubes……CNTs

Counter Electrode……CE

Cyclic Voltammetry……CV

Energy Dispersive X-ray ……EDX

Polypyrrole …… PPy

Field Effect Transistors …… FET

Horseradish peroxidase …… HRP

Poly l-lysine……PLL

Rapid Diagnostic Test ……RDT

Reference Electrode ……...RE

Scanning Electron Microscopy…...……SEM

Screen Printed Electrodes……...SPE

Surface Acoustic Wave……..SAW

Working Electrode ……WE

X-ray Diffraction……XRD

Zeolite Modified Electrode ……...ZME

CHAPTER ONE

INTRODUCTION

1.1 Background

A biosensor is a device that converts biological information into a signal for meaningful purposes. A classic example of a biosensor is the glucometer which is used in our health care centres. The basic biosensor is made up of an analyte, transducer and an electronic system. The analyte (target) is the product under investigation such as cultured cells, human, food and environmental samples. The transducer consists of the biologically active molecule (bio-receptor) coupled to the electrode (electrical interface). A bio-receptor is the probe molecule (DNA, enzymes and many more) that is specifically bound to the target analyte. The electrode is the conductive material that recognises changes in activities of the working cell. This measures the changes in activity on the electrode surface (heat output, distribution of charges and light output). Then finally an electronic system that converts the reaction determined by the transducer into meaningful electrical signals [1].

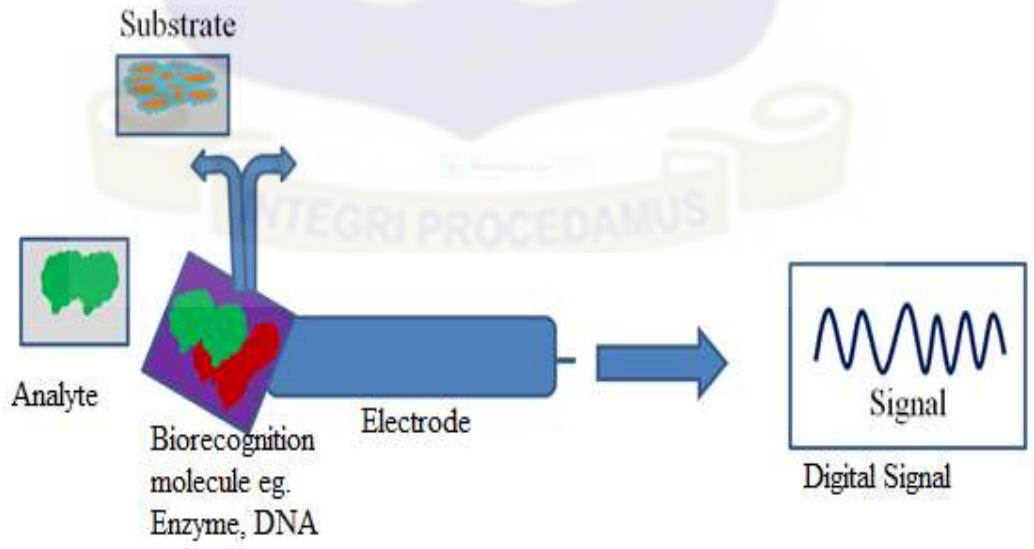

Figure 1: Basic Architecture of a Biosensor.

Electrode surfaces of the sensors must be modified with different nano-technological products such as mercury, carbon, nanotubes and polymers to enable easy immobilisation of the biological molecule to improve its analytical characteristics and reproducibility.

Over the years, mercury has been used as the most suitable material for the modification of electrode surfaces due to its high reproducibility and smooth surface. Although hazardous, the properties of mercury drop electrode led to the Nobel Peace Prize in Chemistry being awarded to Heyrovsky in 1959.

Zeolites have shown great promise, compared to other alumina-silicates and crystalline materials for the modification of electrode surfaces [2]. A particular feature of zeolites is the existence of a network of cavities linked by channels, which provides a large specific surface area, enabling it to trap the biologically active molecules used for biosensor development. Zeolites are distinguished from other porous materials by its pore size variety and ion exchange capacity [2].

The greatest challenge of biosensor fabrication is the immobilization of the biological molecules (for example, antibodies, cells, and enzymes) on the surface of the transducer. Biologically active molecule (for example enzymes) can be immobilized by either covalent binding, entrapment, microencapsulation or cross-linking onto the transducer surface. The disadvantages of these methods are; loss of molecule activity, instability, poor reproducibility of biosensor signals, and toxicity of the compounds which induce the binding [3].

The sensitivity and overall performance of enzymatic biosensors have improved tremendously over the years as a result of the synthesis and incorporation of nanomaterials in their fabrication [4-7]. These materials have excited engineers due to their unique structural, electrical, chemical and mechanical properties [8-11]. In the field of medical device fabrication, there are currently numerous studies describing the use of gold nanoparticles, graphene, zeolites, quantum dots, silver nanomaterials, nanocomposites as well as carbon nanotubes (CNTs) for enzyme immobilization due to certain characteristics ranging from their biocompatibility to fast response times [12-15]. One of the oldest known materials is clay minerals which have been used predominately for curative, industrial and medical applications [16, 17]. They have been widely applied in such fields because of their high colloidal and swelling capacity, surface reactivity, high adsorption, and cation exchange capacity [18-20].

Among the most studied biosensors, are those developed for urea detection using the different sensing methods mentioned earlier [21-25]. Urea is an organic molecule with chemical formula $CO(NH_2)_2$ and is the end product of protein metabolism in the liver. Urea biosensors are of great importance because urea levels in our body are used to diagnose the early stage of renal failure or disorder. Urea undergoes filtration and a series of processes before it is finally excreted. It is, therefore, an important biomarker for detecting renal dysfunction using different testing methods including biosensors.

As a well-studied model system, urea biosensors function on the basis that urea is decomposed by urease to form electroactive species (ammonium ion), accruing to the reaction in equation (1). The electrochemical monitoring of the enzymatically produced NH_4^+ at an appropriate transducer generates the analytical response.

There are currently concerted efforts by the scientific community tailored towards identifying materials that can enhance enzyme immobilization, due to the high demand of biosensors for rapid point-of-care testing.

Biosensors have transducers that are categorised as electrochemical, field effect transistors, optical, piezoelectric surface acoustic and thermal sensors. The type usually depends on the application. Electrochemical transducers can be potentiometric, voltammetric and conductometric. All these measure changes in electrical conductivity and voltage differences occurring at the working electrode (we) surface in comparison to a reference electrode (re).

Electrochemical sensors are made of two or three electrode configurations, with the working electrode (we) and the reference electrode (re), being common to both configurations and the latter having a third electrode called the counter (ce). The two-electrode system is mostly used in areas where prolonged stability of the reference electrode is not needed, hence lowering cost of development. The actual reaction occurs at the working electrode surface where the biological molecule interacts closely with the target analyte and the transducer.

The counter electrode is usually used as a support for the reference electrode to carry charges from the electrolysis reaction to maintain the half-cell potential of the reference electrode. When the biological molecules are immobilised onto the electrode surface, the technique of immobilization determines the working lifespan due to instability, recovery and response time. Although many polymers are good couplers for electrode surfaces, yet their inherent properties denature the biological materials. To overcome these difficulties, zeolites were proposed as carriers for enzyme adsorption. Zeolites are slightly toxic and hardly affected by mechanical, chemical, and thermal effects making zeolite-based biosensors a better option for multicomponent biological samples.

In this work, the effect of crystallization temperature which has significant influence on the pore volume and pore size of zeolite is studied with the immobilization of urease enzyme for the detection of urea.

1.2 Problem and Need Statement

Biosensors have gained a lot of attention due to the demand for the rapid diagnostic test (RDT) which addresses the inconvenience of having to move to a well-established medical laboratory for diseases diagnosis. Test kits are expected to be defined, cost-effective and robust in the diagnoses of diseases. In the development of biosensors, the biological molecule needs to be incorporated in a matrix or on a substrate before being accessed by the analyte. This matrix should be able to retain the biological activity of the biomolecule to enable detection, hence the demand to investigate materials (matrix) such as carbon nanotubes, graphene, polymer, nano-wire and clay minerals which are used as substrates.

Zeolites have proven to have the abilities to keep the biological element in its active state and also improve the analytical sensor response due to some key inherit properties. Zeolites from the commercial markets are expensive and not easy to come by. , However, it can also be synthesized from kaolin; a natural mineral which is readily available in our local settings.

The procedure of obtaining zeolite from kaolin is well established, but the parameters that affect its immobilisation characteristics are not well defined, hence the need to investigate the parameters that affect the syntheses of zeolite from kaolin and study the analytical characteristics of the product using urea as a proof of concept.

1.3 Hypothesis

Zeolites can be synthesized from kaolin deposits in Ghana at different crystallization temperatures. Zeolite-based biosensors can be developed as an electrochemical biosensor with an improved analytical response to the rapid diagnostic test.

1.4 Aim and Objectives

The aim of the project is to develop electrochemical biosensors with zeolite modified electrode (ZME) surfaces, for the detection of urea as a proof of concept. The development process will utilize zeolite synthesized from kaolin deposits in Ghana through alkaline fusion before hydrothermal reaction. The zeolite will then be used to modify the surface of the electrode by drop coating as reported by Kucherenko et al [26]. This would be achieved by carrying out the following activities:

a) Synthesize zeolite from kaolin deposits in Amanfrom, Eastern part of Ghana by crystallizing at different temperatures.

b) Explore the adsorption properties of the zeolite modified electrode.

c) Test the electrochemical behaviour of the zeolite modified electrode using urease enzyme.

The thesis is apportioned into six chapters; chapter one gives a brief explanation of biosensors and materials for its fabrication; chapter two focuses on literature review in the fabrication of a biosensor and techniques employed in biosensor analysis; chapter three vividly explains the materials and methods employed in executing this work; chapter four shows results obtained while chapter five summarizes the results with follow-up discussions; and the concluding part of the thesis is found in chapter six with recommendation for further studies.

CHAPTER TWO

LITERATURE REVIEW

2.1 Introduction

This chapter describes the review of the literature with respect to the development of biosensors and also highlights subjects that are related to the biosensor development which is being reviewed in this respect.

Electrochemical means of detecting target molecules have been shown to have projections in creating miniaturized devices for use in field evaluations. An important consideration towards this development is the immobilisation of different biological molecules on various electrodes such as gold and silver nanoparticles to facilitate their conductivity and linkage to antibodies [27].

Zhengpeng et al established a sensor that braced an analytically useful wide detection range from 0.5 µM to 3.0 mM, with a short response time and an adequate storage stability. This method immobilised urease onto piezoelectric alumina membranes using conductometric response [28].

Zhao and Zhan demonstrated the detection of *Shigella flexneri* using screen-printed electrode (SPE) biosensors. In this work, Horseradish peroxidase (HRP) labeled antibodies to *S. flexneri* was entrapped into a multi-wall carbon nanotubes/chitosan matrix for the capture of *S. flexneri*. The assay showed satisfactory performance with a detection limit

of 2.3×103 μmL^{-1}. A particular feature of the device was safe since it did not involve culture of the pathogen, it proved to be very useful, cost-effective and robust [29].

Also, a urea biosensor was reported where urease was covalently immobilized in a film of electroinactive polypyrrole (PPy) with polyions polyacrylate (PAA) and poly l-lysine (PLL) to make a composite PPy/PAA-urease-PLL film. The doping of PPy with anions rendered an enhanced stability to the electrode. The PPy/PAA electrode showed a selective Nernstian response to change in H^+ ions (pH), which forms the potentiometric basis of the biosensor. The sensor showed a good operational stability and urea detection in the range 0.018–1.8 mg/dl [30].

A potentiometric array-based biosensor has been reported for the detection of urea in the appearance of interferents such as ammonium, potassium, sodium and hydrogen found in a biological matrix. The sensor is an all solid-state type employing carboxylated PVC as the polymeric membrane, having a linear range detection of 10^{-4} to 10^{-2} M urea with a short response time. The bio-electronic tongue was subjected to the analysis of urine samples. Although some discrepancies were observed between real-time and test samples, a similar array-based urea biosensor was further developed by the same group of workers, with creatinine analyte [31].

2.2 Biosensor

Biosensors are known as analytical devices that consist of a biological sensing component; an immobilized biological element comprising of enzymes [32], whole cells, antibodies, tissues, microorganisms, DNA, protein or RNA, and a transducer comprising of either amperometry, potentiometric, thermometric, piezoelectric, surface acoustic wave

(SAW) and optical transducers among others [33]. This changes the biochemical signal into a quantifiable electrical signal such as temperature adjustment, current, potential, absorption of light or change in mass [34].

2.3 Factors That Affect Immobilization

Immobilizing a biological element means fixing the molecule in place so as to avoid movement of that component or the confinement of enzymes to a matrix. There are numerous requirements for successful immobilization of biological elements used for constructing or making biosensors. The method used for immobilization is a requirement that is essential to successful immobilization of biological elements. Each chosen method of immobilization should; not be complex but simple to use, be effectively stable for the immobilization of biological elements on the surface of its transducer, constitute non-toxic environmental factors so as to not disrupt the activity of the biological element, and a chemically inert and highly reproducible host structure during large-scale production [35, 36].

2.4 Methods of Immobilization and Its Effects

Immobilization methods of the biological element include covalent binding, entrapment and encapsulation, crosslinking and adsorption [37-39] or binding to the transducer surface among others [40, 41]. The effective use of these methods depend on the nature of the biological element to be , used, the kind of transducer to be considered, the chemical and physical properties of the analyte and operational conditions of the biosensor. Most importantly, these considerations must permit the biological element to demonstrate efficient action in its immobilized microenvironment [33].

Conditions like toxicity and chemical inertness may directly affect the analytical features of the biosensors, such as sensitivity, reproducibility, selectivity and detection limit, influence on enzyme positioning, entrapment, motion, stability, arrangement and biological activity [42, 43]. Thus, improving the methods of enzyme immobilization is a critical step in biosensor development [44, 45].

Immobilization is a very delicate process and must be well tailored to ensure the efficacy of the biosensor. The option of the most suitable technique depends on the nature of the immobilized material, the transducer and its related detection mode. The finest method of immobilization will depend on where the biosensor would be applied and if it requires maximum sensitivity or stability [46]. The various immobilization methods are well explained below.

2.4.1 Physical Adsorption

Physical adsorption involves the modest deposition of an enzyme on a surface and its attachment through weak bonds. This method has commonly been used to make enzymatic biosensors, because it is simple, with limited loss of immobilized material but its desorption is non-specific [47]. Hence biological elements are denatured after a short while and reproducibility is feasible.

2.4.2 Affinity Immobilization

Affinity immobilization technique is also used to make biological affinity bonds between a stimulated support and a particular protein sequence (for example, biotin, carbohydrate residue, histidine and many others). It permits the biological element to orient in order to evade the deactivation of an enzyme or the blocking of the active site.
This method has been elaborated to immobilize enzymes using processes such as strept, avidin-biotin, and many more [48].

2.4.3 Cross-Linking

Cross-linking method is attractive because it is simple and has the ability to effectively bind biological element chemically. The major setback is its ability to lose activity due to the alteration of the immobilized conformation and the chemical changes of the active site during the process [49-51].

2.4.4 Entrapment

Entrapment method involves the incorporation of an immobilized material in a gel or polymer. This method requires no chemical reaction but rather a high concentration of an immobilized molecule. In this method, polysaccharide-based gel entrapment enzymes (such as chitosan, alginate or agarose) are presumed in contrast to synthetic polymers such as polyacrylamide, because they are biocompatible, nontoxic, provide normal microenvironment to the enzyme and also provide adequate availability to electrons to travel between the enzyme and the electrode [52-53].

Covalent coupling technique is also another prevalent chemical immobilization method that is employed to create enzymatic biosensors. In this method, there is a chemical bond between functional groups of the immobilized material (the enzyme) and those on the support. This method produces no diffusion barrier, has a short response time, is stable, and has a high enzymatic activity. Nonetheless, its demerits are that matrices don't re-generate and are coupled with toxic products [54].

2.5 Immobilization of Biological Molecule

There are numerous sorts of biological molecules that are used for immobilization in developing biosensors. These molecules include complementary DNA, probe, enzymes, antigens, antibodies, oligonucleotides and others. Even though antibodies and oligonucleotides are usually exploited as molecules for immobilization, enzymes are the most frequently used molecular recognition elements in biosensor development. Numerous books, articles and reviews have penned on enzyme immobilization, thus broadcasting thousands of protocols. , in some cases, enzyme immobilization protocols are also based on diverse immobilization techniques. For instance, one can pre-immobilize an enzyme on beads by adsorption, affinity or covalence before entrapping in a porous polymer substrate. Enzyme immobilization is essential in developing competent biosensors with exceptional performances in operational and storage stability, high selectivity, short response time, high sensitivity and high reproducibility [55-59].

Materials for constructing substrate or supports for immobilization include natural and inorganic polymers. Natural polymer supports for immobilization include alginate, pec-

tin, cellulose, gelatin, chitosan, chitin, starch, collagen and many others, whiles inorganic polymer supports for immobilization include zeolite, glass, silica, ceramics, activated carbon, charcoal and many others [60].

Materials used for the immobilization of biological elements include glutaraldehyde and hexamethyl diisocyanate. These form crosslinks between the biocatalytic species, or proteins [61].

2.6 Enzyme Biosensors

Enzyme biosensors are electrochemical biosensors that employ enzymes as the probe molecules and have become part of the most adopted type of biosensor for health diagnosis, food industry, and environmental monitoring. The biomedical field is the foremost area in biosensor applications, such as monitoring blood glucose levels in diabetics with glucose biosensors (glucometer). Also, dependable recognition of urea has prospective tenders for detecting renal failure or disorders.

The scientific community has focused on the development of biological molecule immobilisation because the procedure for the immobilization of the probe molecule has great influence on the analytical response (limit of detection, sensitivity, reproducibility, selectivity and many more) of the sensor. Enzyme immobilization on the transducer surface is the most essential stage in biosensor fabrication because the enzyme is the probe molecule [62].

2.7 Zeolites for Biosensors

Zeolite-enzymes biosensors have gained immense popularity due to their peculiar properties such as high specific surface area that can be altered using organic and inorganic groups, their shape, charges, and size selectivity, their chemical stability, insolubility in organic solvents, ability to tolerate to microorganisms and resistance to harsh experimental factors [63-65].

2.7.1 Effect of Zeolite Synthesis on Immobilization

Zeolite synthesis is a very sensitive method, in that, controlling variables such as temperature, aging, mode of crystallization, conditions are critical to obtaining a pure crystalline zeolite material and can affect its morphology. These synthetic zeolites may have different properties based on all the variables listed above. The pore diameter, the pore volume and surface area may affect the amount of biological element immobilized and the release of that biological element.

Furthermore, even the elemental composition, the atomic structure of the zeolite formed and the morphology could greatly influence its effectiveness in electrochemistry. Various protocols have been explored in zeolite synthesis with the most common being fusion and hydrothermal methods [66] using controlled crystallization temperature and media [67]. These methods have effectively been used in making zeolite nanoparticle from kaolin [68, 69], coal fly ash [70-74], lignite fly ash [75] and rice husk ash [76, 77] among others.

2.8 Electrochemistry in Biosensing

Measuring electrical signals from activities of biological reaction is electrochemistry. Here, a bioelectrochemical component works as the main transduction element. Electrochemical sensing in biosensors normally needs a working electrode, a reference electrode and a counter or auxiliary electrode.

Over the past decades, several sensing theories and devices have been established with the most widely used traditional techniques being cyclic voltammetry, chromo potentiometry, chrono-amperometry and others. Cyclic voltammetry is one of the most generally used forms of electrochemical sensing. This is normally employed in obtaining information about the redox potential and electrochemical reaction rates of analyte solutions. In this process, voltage is measured between the reference electrode and the working electrode, whereas current measured is between the working electrode and the counter electrode. Measurements acquired are then plotted as current versus voltage, to generate wave form referred to as a voltammogram [78]. The measured values of current and voltage are used in the estimation of analyte concentration.

2.8.1 Electrodes Materials for Biosensing

There are numerous electrodes incorporated with transducers for biosensing, such as gold, silver, stainless steel, platinum, nickel, carbon nanofiber, diamond and others. Platinum, gold, silver, stainless steel and carbon are commonly used to prepare electrode structures and supporting substrates. These metals have long been incorporated in electrochemical electrodes due to their superb electrical and mechanical properties [79]. They do not have direct intimacy with the biological molecule but are able to transduce

the reaction through the incorporated substrate which are normally polymers, nanotubes and zeolite material with inert properties.

These materials exhibit good electrical properties which makes them ideal for biosensor fabrication, by the act of transmitting the chemical reaction occurring at their surface to measurable electrical signals that are used in diagnosis.

2.9 Types of Biosensors and Their Uses

Types of biosensors such as conductometric, potentiometric, electrochemical, amperometry, optical, calorimetric biosensors and others [68, 80], can be used to determine the amount of glucose in the blood, to detect renal diseases by monitoring urea concentrations in the body and sensing hybridized or single-stranded DNA.

Also, cholesterol biosensors have become indispensable in the clinical diagnoses for estimating cholesterol in patients, whiles environmental biosensors show variations in alarm when harmful gases such as ammonia or formalin are present in high or low concentrations in the environment. Also, food biosensors are used for detecting compounds such as glucose, sucrose, citric and ascorbic acid and many more in food for quality control purposes [81].

2.10 Rationale

The recent rise in epidemics has affirmed the need for the public health authority to gain interest in the readiness for a solution to curb disease occurrences, especially in the developing world. Many advanced techniques are still not feasible in low and middle-

income countries (LMIC) where they are most needed in the past few decades. Clearly, these performance parameters would offer an alternative diagnostic approach to healthcare in developing countries where resource constraints hinder the implementation and accessibility of sensitive but expensive diagnostic testing management.

This work, therefore, seeks to develop easy-to-use and affordable diagnostic tools to help support the fight by the public health authority in confronting the challenges of low and middle-income countries.

Electrochemical devices that are based on the simple principle would improve the quality of laboratory diagnosis of diseases and afford desired clinical information in a simpler, faster, and cheaper manner such as the glucometer for sugar test.

CHAPTER THREE

MATERIALS AND METHODS

3.0 Introduction

This chapter gives information on the basic materials used in the execution of the work as well as the equipment used and sample preparation procedures.

3.1 Materials

Kaolin deposits from Amanfrom in the eastern part of Ghana was collected as the basic material for the production of the proposed zeolite as shown in figure 2. Sodium Hydroxide (NaOH) Pellets with 99% purity was used as the base to fuse the kaolin in order to form the zeolite. Phosphate buffered saline (PBS), pH 7.4, was obtained from Sigma-Aldrich, St. Louis, USA and used as a medium for the zeolite synthesis. The urease enzyme (urease active meal from Jack beans) was obtained from Sigma-Aldrich, St. Louis, USA and is used for the hydrolysis of urea. The target analyte; urea was obtained from Department of Chemistry, University of Ghana. Deionized water was also obtained from Millipore, Bedford, MA, USA purposely for the preparation of all solutions in the execution of the research.

A pair of gold electrodes was obtained from Griffin and was used to create the bioelectrode. A hot plate was obtained from IKAMAG RCT to be used to dehydrate the zeolite paste that was deposited on the gold electrodes surface. A furnace was also purchased from Thermo-Scientific, Waltham, MA, USA and used for high-temperature heating of

the samples. Finally, a Metrohm AutoLab PGSTAT 204 electrochemical device was used to detect the working cells' current.

Figure 2: Harvesting of the kaolin from Amanfrom village in the eastern part of Ghana.

3.2 Methods

The following describes the procedure used in the synthesis of the zeolite from kaolin and the steps followed in modifying the surface of the gold electrodes for the immobilization of the biological molecule (urease enzyme). Also, a stepwise procedure of impregnating the urease enzyme in the monolayers of the zeolite films are described.

3.2.1 Sample Preparation (Zeolite Synthesis)

The zeolite synthesis was carried out using a combined approach involving alkaline fusion followed by the hydrothermal reaction as stated by Ríos et al. 2007 [68]. Briefly, 20 g of kaolin was ground into granules and sieved with 100 µm and 63 µm sieves simultaneously (with 100 µm placed on top of the 63 µm). The residue in the 100 µm was then disposed of and the fine particles after the 63 µm sieve were weighed on a scale to obtain 15 g as depicted in figure 3a & b.

(a) (b)

Figure 3: (a) Depicts sieving of grounded kaolin, (b) Fine grains of kaolin sieved with 63 µm.

The fine grade particles obtained and weighed after sieving was then poured into a crucible and calcined in a Thermo-Scientific furnace set at 650 °C for 120 minutes to obtain metakaolin as depicted in figure 4 [68].

(a) (b)

Figure 4: (a) Shows crucibles filled with kaolin and placed in a furnace, (b) shows the furnace used to heat the kaolin to the desired temperature to obtain metakaolin.

In order to have equal working and external conditions, all the kaolin samples were calcined in the same furnace at the same time. The metakaolin which appears in lumps as a result of decomposition as shown in figure 5 was ground and mixed with sodium hydroxide (NaOH) powder in a mass ratio of 2:3 (Kaolin: NaOH, w/w).

Figure 5: Samples of alkaline fused metakaolin for the five different crystallization temperatures.

The ensuing mixture was fused at 600 °C for 120 minutes in a furnace. The product obtained as a result of the alkaline fusion followed by the hydrothermal reaction was then ready to be mixed into a measured amount of deionized water. The mixture was then crushed into fine powder in a mortar to increase its reactivity with distilled water. The fine powder was then mixed with distilled (deionized) water in the mass ratio of 1:5 (powder: water, wt/wt) in a beaker and stirred to obtain a homogeneous mixture as shown in figure 6. The homogeneous mixture was kept at room temperature for 24 hours for gelation to take place since nucleation is highly affected by the aging time and temperature.

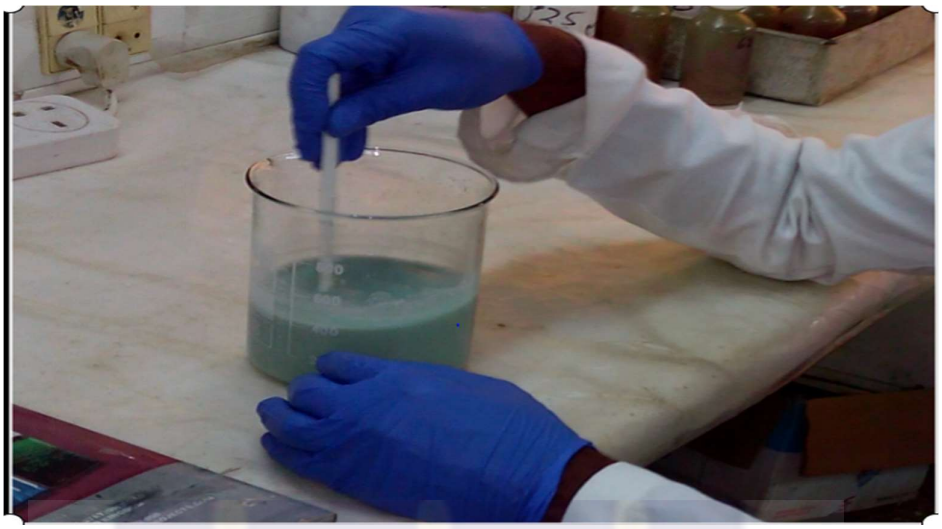

Figure 6: Alkaline fused metakaolin added to deionized water.

The resulting gel was then crystallized at temperatures, 60 °C, 70 °C, 80 °C, 90 °C and 100 °C for 24 hours in an oven. The newly formed crystalline material was then removed from the oven. The reaction process was terminated by cooling in cold water. All the materials crystallized at these different temperatures had an average pH of 13.3, which makes them hazardous to handle. The pH was then reduced by constant filtration with deionised water.

The samples were then dried in an oven at 60 °C for 24 hours. They were weighed, packed and labelled by their respective crystallization temperatures in falcon tubes as shown in figure 7a, with figure 7b depicting how the samples were packaged for bio-physical characterisation, namely, X-Ray Diffraction (XRD), Scanning Electron Microscopy (SEM), Energy Dispersive X-Ray (EDX) and Brunner Emmett Teller (BET). These were used in the characterisation of the crystalline materials formed and the elemental compositions of the end products were also identified.

(a)

(b)

Figure 7: (a) Synthesized zeolites at different crystallization temperatures, (b) Packaged crystalline material for biophysical analysis.

3.3.0 Biophysical Characterization

3.3.1 X-Ray Diffraction (XRD)

XRD is used in the identification of unknown crystalline materials or composites by generating information on the crystalline components present in the material. The XRD was performed with a PanAnalytical Diffractometer as shown in figure 8 using CuKα radiation at 2θ, scanning from 5 to 50 degrees in steps of 0.05 degrees, with a tube voltage of 45 kV and a current of 40 mA. The d-spacing (ds) of the material is generated and an

automated search engine compares the unknown ds to known ds, since each mineral has a unique set of d-spacing. This provides an identification of the unknown sample that is shown in Chapter 4.

Figure 8: XRD equipment used for diffraction analysis at the University of Ghana, Department of Physics.

3.3.2 Scanning Electron Microscopy (SEM)

SEM involves the interaction of electrons with materials of interest to produce various signals which are then used to obtain information about the surface morphology. SEM micrographs in this study were obtained at an accelerating voltage of 10 kV using a JEOL JSM-7100F field emission scanning electron microscope. Approximately 50 µm of colloidal graphite (Agar Scientific Ltd, Stansted, UK) was uniformly spread on an aluminum stub. Each powdered sample was then deposited on the sticky colloidal graphite and excess particles were removed by tapping the stub sideways followed by blowing with an aerosol duster. In this work, the topography of the crystalline material was observed.

3.3.3 Energy Dispersive X-Ray (EDX)

This is an x-ray technique used for the elemental analysis or chemical characterization of a sample. Data from this technique is then used to analyse the energy spectrum in order to determine the abundance of specific elements. The EDX spectra and the elemental composition of each sample were obtained at an accelerating voltage of 10 kV using a JEOL JSM-7100F field emission scanning electron microscope equipped with a Thermo-Scientific UltraDry EDX detector. Each sample was then removed from the scanning electron microscope (SEM) machine after the EDX analysis and sputter-coated with three nanometres of gold. For the scope of this work, this technique was used to estimate Si: Al ratio by indicating the amount of each element present in the material of interest.

3.3.4 Brunner Emmett Teller (BET)

BET entails the physical adsorption of gas molecules on a solid surface and serves as the basis for measuring the specific surface area, pore size distribution, particle size and dissolution rate. This information is obtained and used to predict the number of biomolecules that could be entrapped in the voids of the zeolite. Nitrogen adsorption measurements were performed at −196 °C on a micrometric ASAP 2020 volumetric adsorption analyser. Before the analysis, the samples were degassed under vacuum at 200 °C for 120 minutes in the port of the adsorption analyser. The result of this test is tabulated in the ensuing chapter.

3.4 Electrode Modification

A pair of gold electrodes with a dimension of 3 mm x 40 mm and identical electrical characteristics were modified locally at the University of Ghana, Department of Physics.

A thin film of zeolite was deposited on the gold electrode surface after heating the thin film of the paste on the electrode surface.

The gold electrode was acting as the transducer, with one open-ended cylindrical dimension obtained from Griffin. The active zone of the gold transducer was 3 mm x 40 mm (one open-ended cylinder) which gave an active surface area of 384.06 mm^2 as depicted in figure 9 below. This modification was done in order to bake the transducer on a hot plate. Two identical gold electrodes were used to bring half-cell potential to zero. The surface of the transducer was enhanced to enable the adsorption of the biomolecule (urease) onto its surface and for subsequent bio-recognition of the substrate (urea).

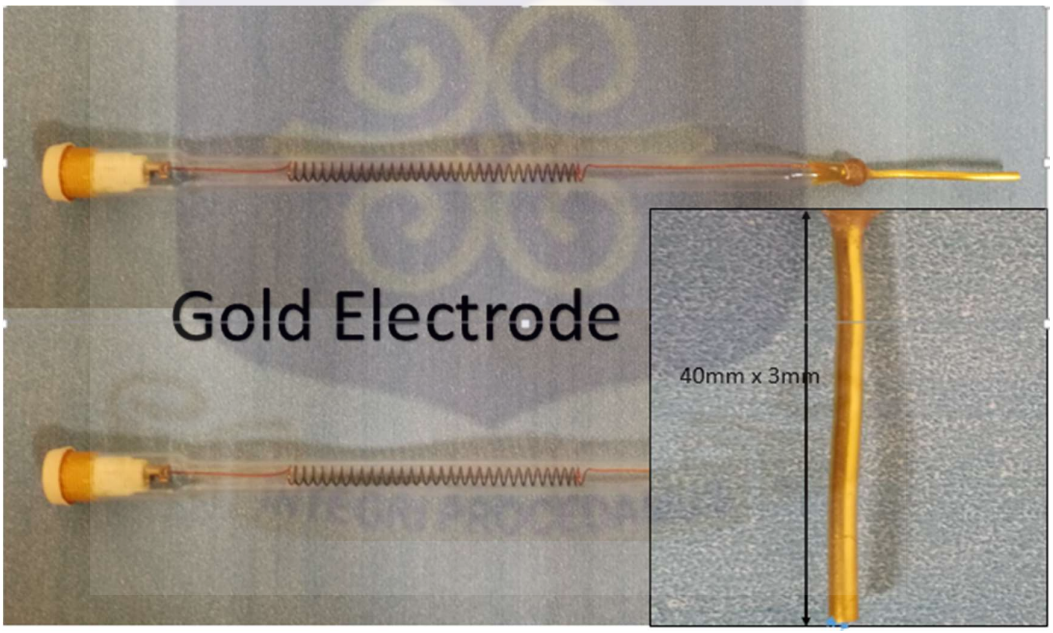

Figure 9: Modified Griffin gold electrode.

3.5 Drop Coating

To modify the surface of the gold electrode with the zeolite, the following procedure was followed to ensure the deposition of the zeolite membrane on the active zone of the surface of the gold electrode. This was achieved by mixing 0.5 g of Zeolite X (Na) in 0.25 ml of 0.1 mM phosphate buffered saline (PBS), pH 7.4 to obtain a paste. The active surface areas on the pair of electrodes were dipped in the paste for a maximum of 90 minutes to enable adhesion of the paste onto the surface of the electrode under room temperature as shown in figure 10 below.

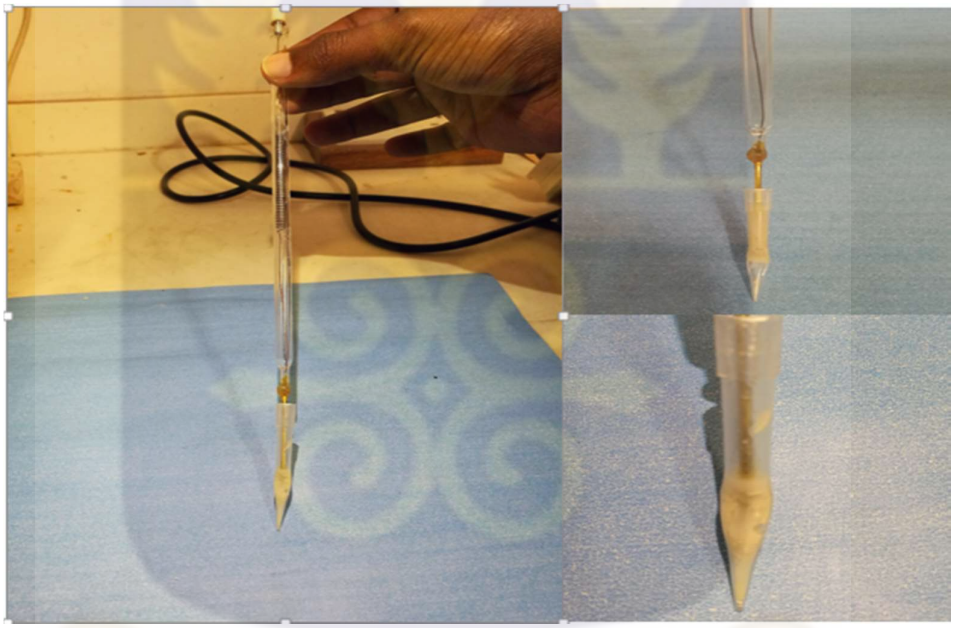

Figure 10: Active zone of gold electrode dipped into the zeolite paste.

The zeolite modified gold electrode (GE) surface was placed on a heat block set at 200 °C for five minutes as shown in figure 11. This was done to dehydrate the layer of zeolite on the surface of the gold electrode without changing the orientation and the characteristics of the electrode.

Figure 11: Zeolite modified gold electrode placed on heat block set at 200 °C for dehydration.

This left a thin layer of zeolite spread over the active zone of the electrode as shown in figure 12 below. Both the working electrode and the reference electrode were dipped in the zeolite paste for all the crystallization temperatures.

Figure 12: Thin layer of zeolite deposited on the gold electrode active zone after dehydration.

3.5 Immobilization of the Biomolecules

One of the two zeolite modified gold electrodes was then dipped into urease and bovine serum albumin (BSA) solutions respectively for optimal absorption. The reference electrode (RE) pre-coated with Zeolite X (Na) at a particular crystallized temperature was dipped into 10% BSA solution for absorption onto the pore structure of the zeolite. The working electrode (WE) which was also pre-coated with Zeolite X (Na) of the same crystallization temperature was dipped into 2 ml of 10% urease solution (1 g to 10 g of PBS). The two electrodes were air dried for 20 minutes at room temperature in order to maintain the stability of the proteins. The inertness of the zeolite maintained the biomolecules in a stable state. The electrodes were then washed off in a working buffer to remove all adsorbed biomolecules from the surface of the electrode.

3.5.1 Second Drop Coating

The modified gold electrode with a layer of zeolite spread over it, as shown in figure 12 above, was subsequently dipped into urease solution and again dipped into the same zeolite paste, to have the enzyme covered with another layer of zeolite.

After this coating, the electrode was then air dried at a temperature of 24 °C for 12 hours to keep the enzyme in its active state, since higher temperatures above 40 °C will denature the enzyme. The electrodes were then washed off in a working buffer to remove all adsorbed biomolecules from the surface of the electrode.

3.6 Electrochemical Measurements

Cyclic voltammetry (CV) measurements were taken using Metrohm AutoLab PGSTAT 204 interfacing a computer with NOVA 2.0 as the control setup in figure 13 below and operating software using Microsoft Windows 10 operating system with operational parameters as displayed in **table 1** below.

Table 1: The parameter set used to generate the Cyclic Voltammetry (CV) measurements.

Parameter	**Value**	**Unit**
Step voltage	0.00244	Incremental V
Start Potential	0	V (volts)
Upper vertex potential	-1	V_{ref}
Lower vertex Potential	1	V_{ref}
Scan rate	100	mV/s
Working electrode (WE) current	1 mA–100 nA	A

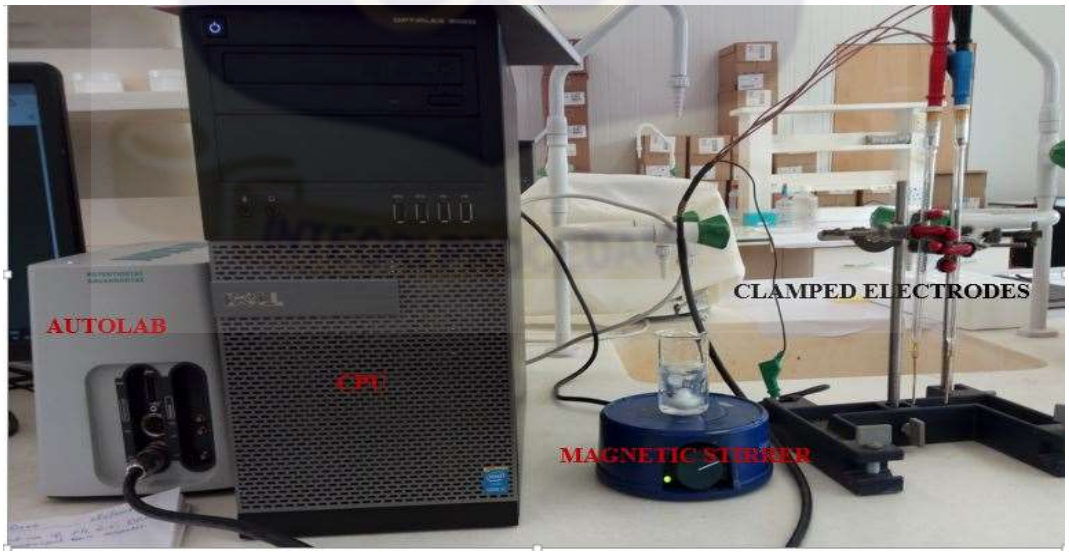

Figure 13: Cyclic voltammetry setup, AutoLab PGSTAT 204, magnetic stirrer and bare gold electrodes.

The zeolite modified gold electrodes (ZME) were dipped into the working cell containing 20 ml of 0.1 mM PBS solution. 1 mL of different concentrations of urea solution namely, 0.1, 0.2, 0.3, 0.4, 0.5, 0.6, 0.7, 0.8, 0.9 and 1.0 mM were added to 10 different beakers containing 20 ml of 0.1 mM PBS at pH 7.4 in 25 ml working cells respectively. The resulting mixtures were homogenized with a magnetic stirrer for 180 seconds. The electrodes had similar treatments for each concentration of urea. The 10 different concentrations were chosen in order to plot a standard curve from their conductivity behaviour. The standard curve could be used to determine the concentration of unknown urea solutions.

For the scope of this work, the electroanalytical method used to study the analyte is cyclic voltammetry. In this technique, the working cell current is measured while an activity that is occurring in the working cell between the urea and the urease alters the working cell's potential. This causes potential changes that are transduced by the electrode into a current signal that is measured and interpreted as equivalent concentration.

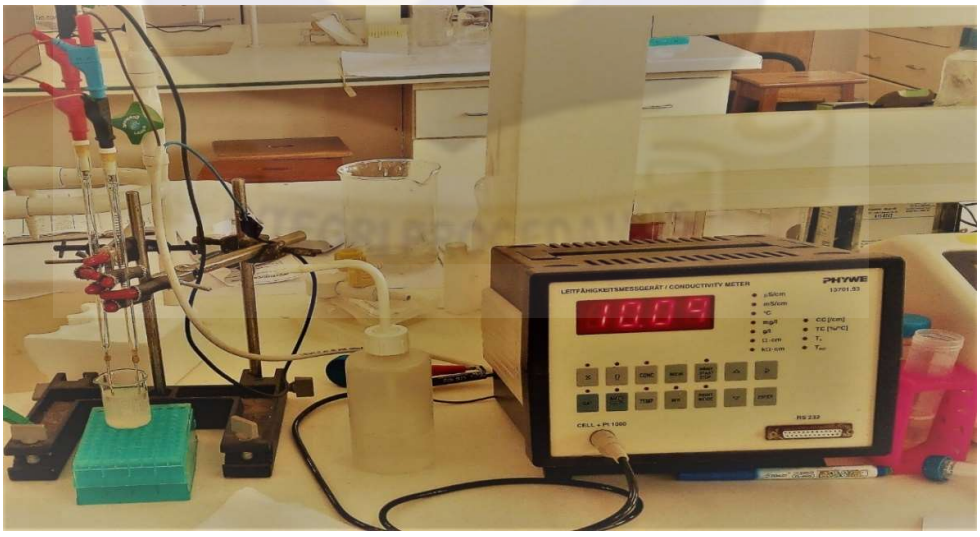

Figure 14: Phywe concentration & conductivity meter for analysing the conductance of the biosensor thus developed.

The molar conductivity (ohm-1cm2mol-1) is also measured with Phywe conductivity meter as shown in figure 14. Conductivity depends on the availability of ions and the mobility of ions. As concentration increases, there is an increased number of ions but their mobility is restricted by the little available space to travel. This makes molar conductivity as described by Debye-Huckel-Onsager equation for weak electrolytes such as ammonia, acetic acid, tartaric acid and many more decrease with increasing analyte concentration. The molar conductivity test was performed in order to obtain a standard curve that could be extrapolated to determine the concentration of unknown urea solution.

3.6.1 Cyclic Voltammetry (CV)

Cyclic voltammetry is a very popular technique for electrochemical studies. It is useful for obtaining information about fairly complicated electrode reactions. It is also used to analyse the current at the working electrode which is used to estimate the analyte concentration. The data from a CV is used to plot a graph called voltammogram as shown in figure 15 below.

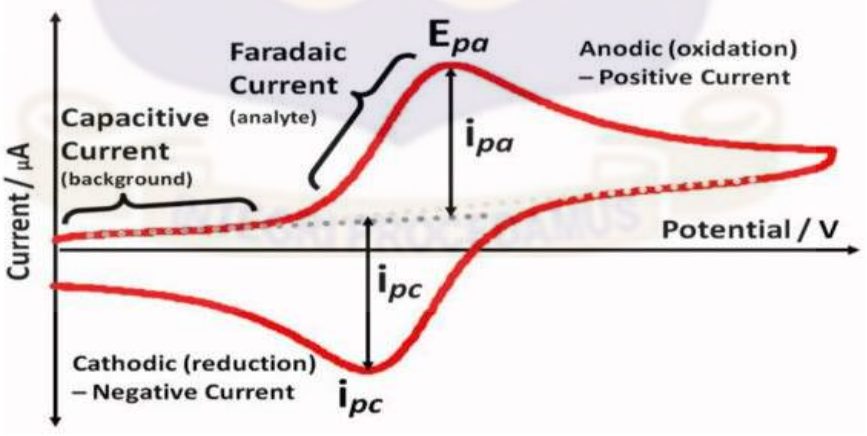

Figure 15: A voltammogram of a reversible analyte

All Electrochemical experiments were conducted using VSP-300 Multichannel Potentiostat/Galvan Stat/EIS with a two-electrode system consisting of identical modified gold electrode. A BioLogic electrochemical analyser with EC-Lab® software was used for the acquisition of data and experimental control. The data analysis was carried out using the EC-Lab® software to identify the peak anodic and cathodic currents which was then used to estimate the concentration of the analyte with respect to Randles-Sevcik Equation (Equation 2).

The peak anodic (i_{pa}) and cathodic (i_{pc}) currents were used to estimate the concentration of the analyte under study. The solution was subjected to a redox reaction which then causes electrical changes (resistance or current) near the surfaces of the electrode. The cyclic voltammetry behaviour of the various zeolite modified gold electrodes (ZME) was studied using urease enzyme as the probe specie against urea in a PBS solution. The bio-recognition signal, in this case, current (I), is proportional the concentration of the analyte by the Randles-Sevcik Equation (Equation 2).

$$i_p = (2.68 \times 10^5)\ ACn^3/2(DV)^{1/2} \quad \ldots\ldots (2)$$

"Where, i_p = Peak Current value (Anode & Cathode)

A = Electroactive Area of the Electrode

C = Concentration of probe molecules in the solution

D = Diffusion Coefficient of the molecules

V = Scan Rate (Potential)

n = number of electrons involved in the Redox Reaction"

The molar conductivity of urea hydrolysis by urease was obtained from the cyclic voltammogram (CV) as depicted. The plot of the current (A) at the working electrode versus the potential applied (V) gives the cyclic voltammogram of the reaction, when the probe molecule (urease) reacts with the substrate (urea) at the surface of the electrode. The resulting electrical changes generate data that is used to plot a voltammogram. In this work Origin Pro 9.0 64-bit software was used in the analysis of the data and the plotting of the voltammogram.

3.7 Exponential Regression Fits and Molar Conductance Curves

The peak current and concentration of urea was used to plot exponential decay regression fits and molar conductance curves using Origin Pro 9.0 64 Bit software. This was done to find a relationship between the conductance of each zeolite modified electrode against their molar concentration. And use to determine the zeolite that gave the best analytical response.

CHAPTER FOUR

RESULTS

4.0 Introduction

This chapter shows data acquisition from the biophysical characterisation and cyclic volt-ammetry experiments performed by the already mentioned equipment.

4.1 Biophysical Characterization

4.1.1 X-Ray Diffraction (XRD)

The results obtained from the X-Ray Diffraction (XRD) confirmed Zeolite X (Na) as the crystalline material that was formed. This was because the signature peaks obtained from the XRD matched with that of Zeolite X (Na) for all the different crystallization temperatures. The crystalline materials were labeled according to each crystallization temperature; this was because the overall yield of the crystalline material was Zeolite X (Na). It was labelled as follows, Zeolite X (Na) 60 °C, Zeolite X (Na) 70 °C, Zeolite X (Na) 80 °C, Zeolite X (Na) 90 °C and Zeolite X (Na) 100 °C respectively. Hence, they will be referred to as indicated above.

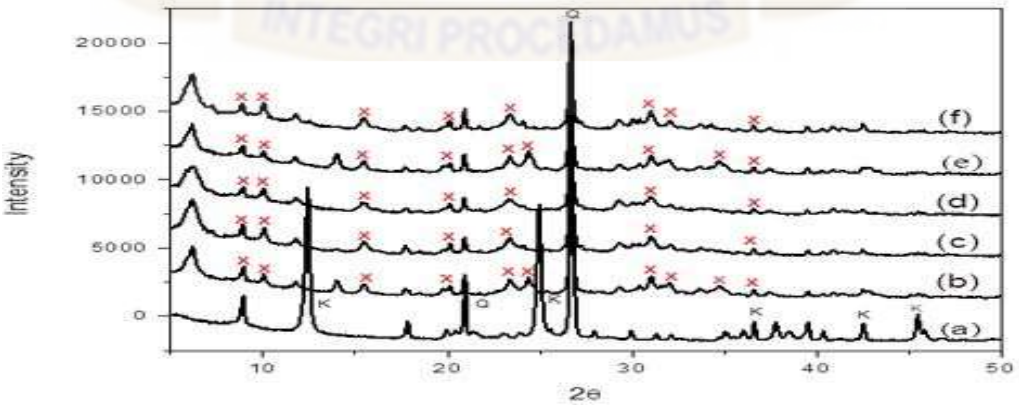

Figure 16: XRD of graphs of Zeolite X (Na) synthesized at various temperatures.

"K" and "Q" denote kaolinite and β-quartz peaks respectively with signature peaks of Zeolite X (Na) indicated in red as "x". The graphs labelled a-f represents kaolin, Zeolite X (Na) 60 °C, Zeolite X (Na) 70 °C, Zeolite X (Na) 80 °C, Zeolite X (Na) 90 °C, Zeolite X (Na) 100 °C respectively.

All the peaks labeled "x" in figure 16 are confirmed signature peaks of Zeolite X (Na). The overall yield of zeolite from the different crystallization temperatures was the same with a significant difference only being the peak intensities of the fingerprint peaks of the Zeolite X (Na). It can be concluded that crystallization temperature did not have an effect on the overall yield of zeolite formed, but rather the intensity of the peaks (area under the peaks) as demonstrated by C. Belviso et al [82].

4.1.2 Scanning Electron Microscopy (SEM)

The result of SEM displayed in Figure 17 below at a scale of 50 microns.

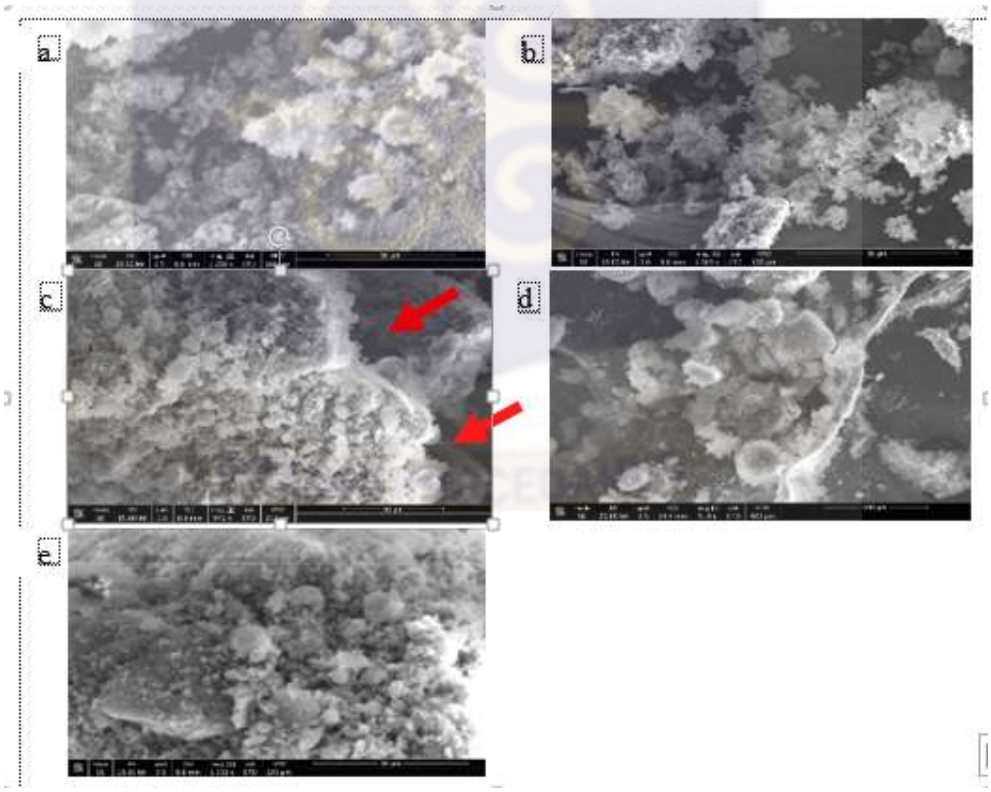

Figure 17: SEM images of Zeolite X (Na) synthesized at 60 °C, (b) 70 °C, (c) 80 °C, (d) 90 °C and (e) 100 °C with scale bar = 50 micron.

Most nano-porous materials such as zeolites are insulators and are particularly susceptible to electron-beam damage and charging. For this reason, no accurate surface observations have yet been performed. If the accelerating voltage is increased in an effort to acquire more detailed information, although the resolution increases, primary electrons penetrate the sample, yielding little surface information. However, our samples had identical crystal structures, differing only in the aluminum content.

4.1.3 Energy Dispersive X-Ray (EDX) and Brunner Emmett Teller (BET)

The Energy Dispersive X-Ray (EDX) results were compared and the respective Si: Al ratios were calculated and shown in the table below. The Brunner Emmett Teller (BET) results revealed distinct pore sizes, diameters and surface area for Zeolite X (Na) crystallized at different temperatures.

Table 2: Characteristics of Zeolite Synthesized at Different Crystallization Temperature

Zeolite	Si:Al ratio	Pore diameter (nm)	Surface area (m^2/g)	Pore Volume (cm^3/g)	Average Crystallite size (nm)
Zeolite X (Na) 60 °c	1.25	2.23	64.32	0.012	44.32
Zeolite X (Na) 70 °c	2.00	2.45	67.77	0.017	39.77
Zeolite X (Na) 80 °c	1.23	4.21	295.25	0.762	35.30
Zeolite X (Na) 90 °c	2.25	1.92	113.14	0.061	36.10
Zeolite X (Na) 100 °c	1.23	4.92	389.43	0.837	44.30

4.2 Effect of Base Materials

The voltammetric behaviour of the bare electrode in the buffer solution with all the reagents w studied and shown in figure 18, this was performed in order to observe their effect on the electrochemical reaction using the setup from **figure 12** in chapter 3.

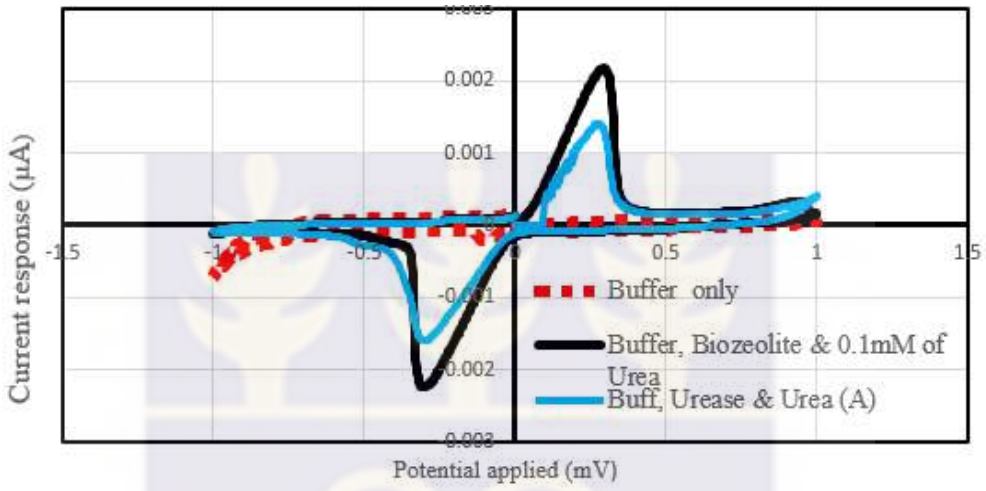

Figure 18: Shows the voltammetric behaviour of electrodes and reagents.

The voltammogram of the buffer solution, urea and urease enzyme with the bare electrode were studied to ascertain its effect on the experiment. The buffer solution did not give any significant anodic peak current after the runtime. Also, urease enzyme on the bare gold electrode gave a peak current of an approximately 0.0014 µA after urea was added to the working cell. After the modification of the surface of the gold electrode with Zeolite X (Na), there was an indication of an increase in peak anodic current of 0.0021 µA as shown in figure 18. This compared with the biomolecule that was adsorbed on the bare electrode, indicated an electrocatalytic activity on the electrode surface. Zeolite X (Na) also permitted increased levels of the bio-receptor to be immobilised, which resulted in high-level electron transmission and improved analytical response.

4.2.1 Cyclic behaviour of Zeolite X (Na) at different crystallization temperature.

The cyclic voltammetry (CV) behaviour of the Zeolite X (Na) 60 - 100 °C was then studied with urea concentrations from 0.1 mM - 1.0 mM. The figures 19-23 below show the unique behaviour of the zeolite prepared with urea concentrations from 0.1 mM to 1.0 mM. In this work, cyclic voltammogram results for urea 0.1, 0.5 and 1.0 mM and the overall behaviour of the 10 concentrations of the biosensor are depicted in the ensuing pages.

The voltammogram shows the analytic behaviour of the biosensor that was developed for all the different crystallisation temperatures. The peak anodic current was calculated from the baseline of zero to the highest peak of the reaction within the runtime. This was indicated in black as a trace line from to the highest point (peak) of the plateau to the x-axis.

4.2.2 Cyclic voltammogram of bioelectrode with Zeolite X (Na) 60 °C in selected urea concentrations.

The peak anodic current which is proportional to the concentration of urea that is hydrolyzed by the urease enzyme on the bioelectrode surface with Zeolite X (Na) 60 °C for selected urea concentrations of 0.1 mM, 0.5 and 1.0 mM are as shown in figure 19 a-c respectively. All the 10 concentrations (0.1 mM – 1.0 mM) of urea for the same zeolite are depicted in figure 19 d, with the various determined anodic currents tabulated in table 3.

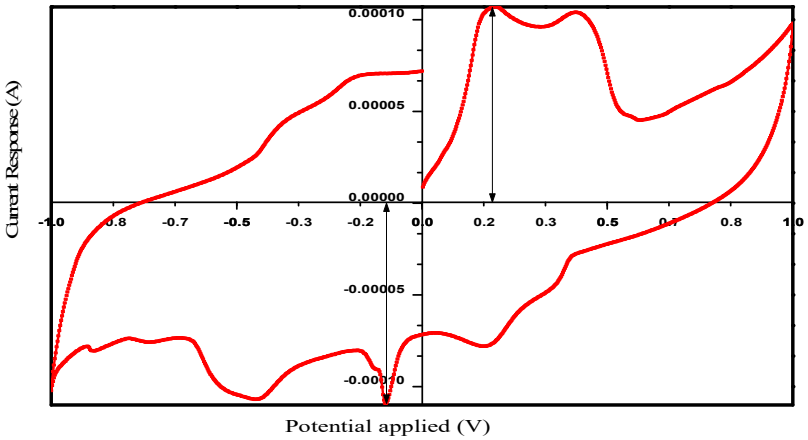

Figure 19: (a) Cyclic voltammogram of 0.1 mM urea.

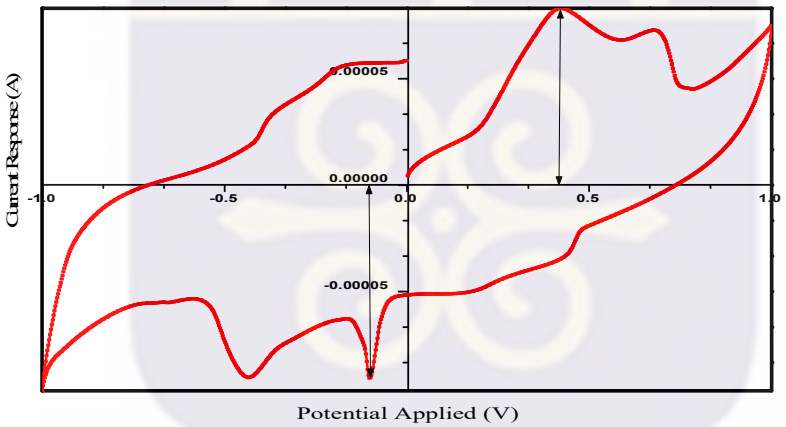

Figure 19: (b) Cyclic voltammogram of 0.5 mM urea.

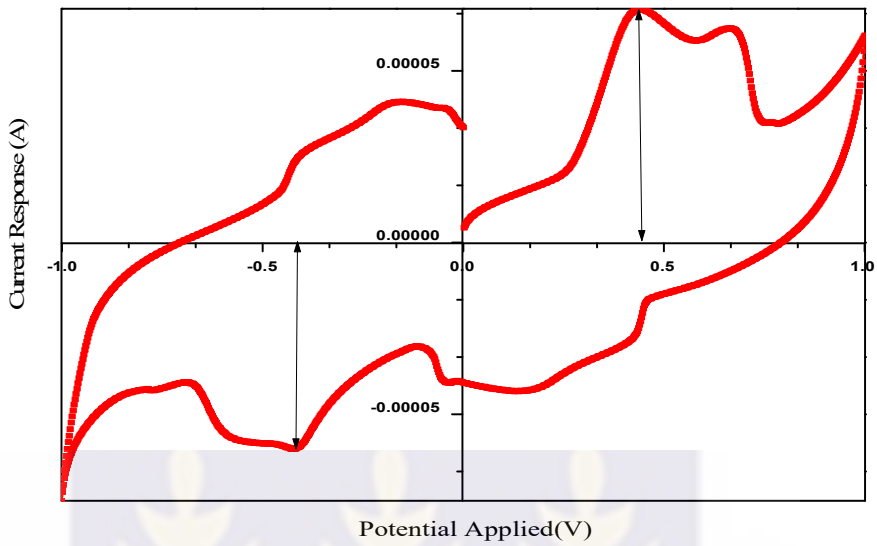

Figure 19: (c) Cyclic voltammogram of 1.0 mM urea.

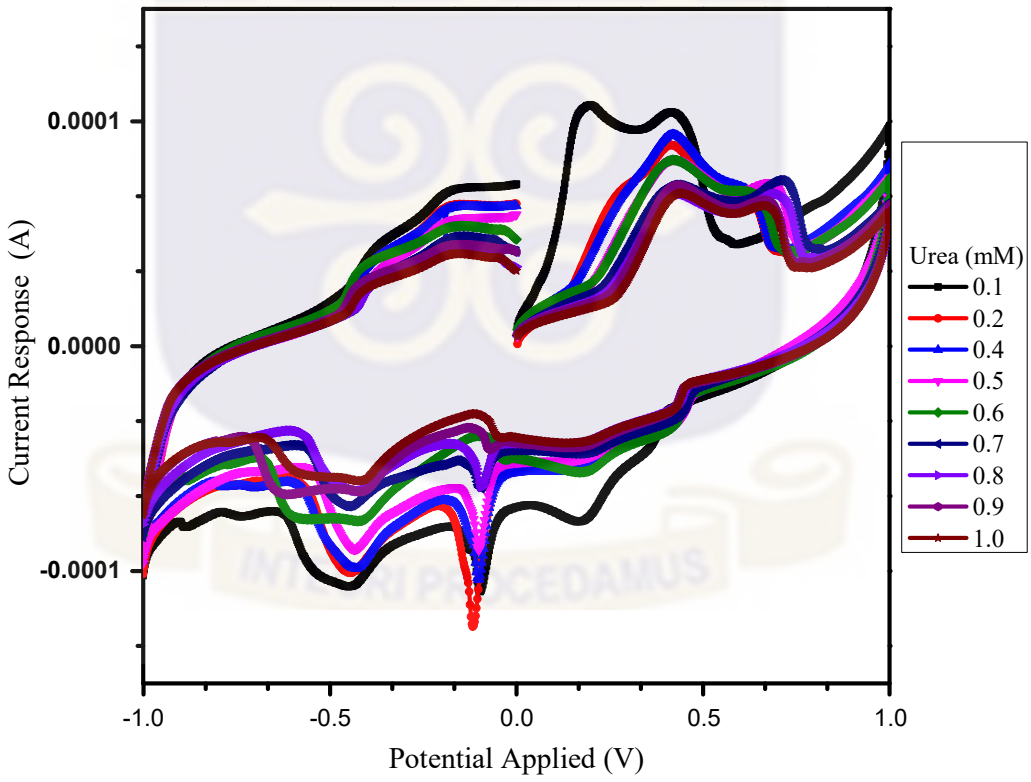

Figure 19: (d) Cyclic voltammogram of 0.1-1.0 mM urea superimposed for Zeolite X (Na) 60 °C modified biosensor.

4.2.3 Cyclic voltammogram of bioelectrode with Zeolite X (Na) 70 °C in selected urea concentrations

The peak anodic current which is proportional to the concentration of urea that is hydrolyzed by the urease enzyme on the bioelectrode surface with Zeolite X (Na) 70 °C for selected urea concentrations of 0.1 mM, 0.5 and 1.0 mM are as shown in figure 20 a-c respectively. All the 10 concentrations (0.1 mM – 1.0 mM) of urea for the same zeolite are depicted in figure 20 d, with the various determined anodic currents tabulated in table 3.

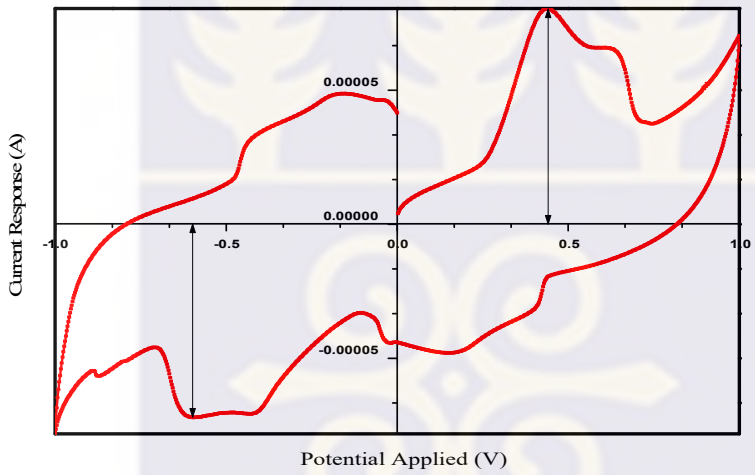

Figure 20: (a) Cyclic voltammogram of 0.1 mM urea.

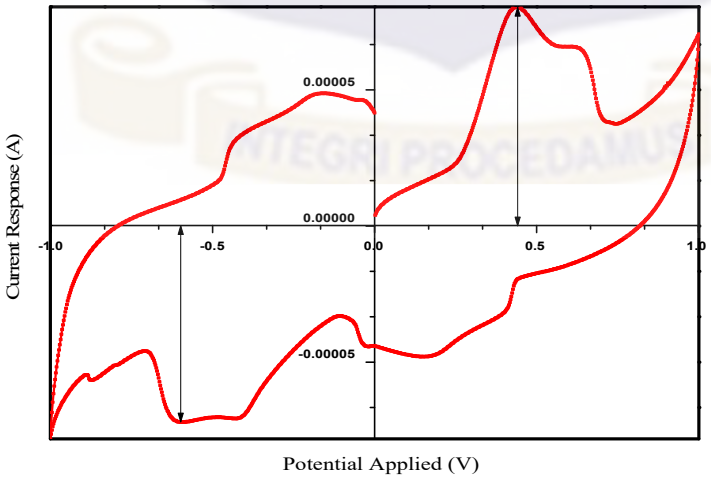

Figure 20: (b) Cyclic voltammogram of 0.5 mM urea

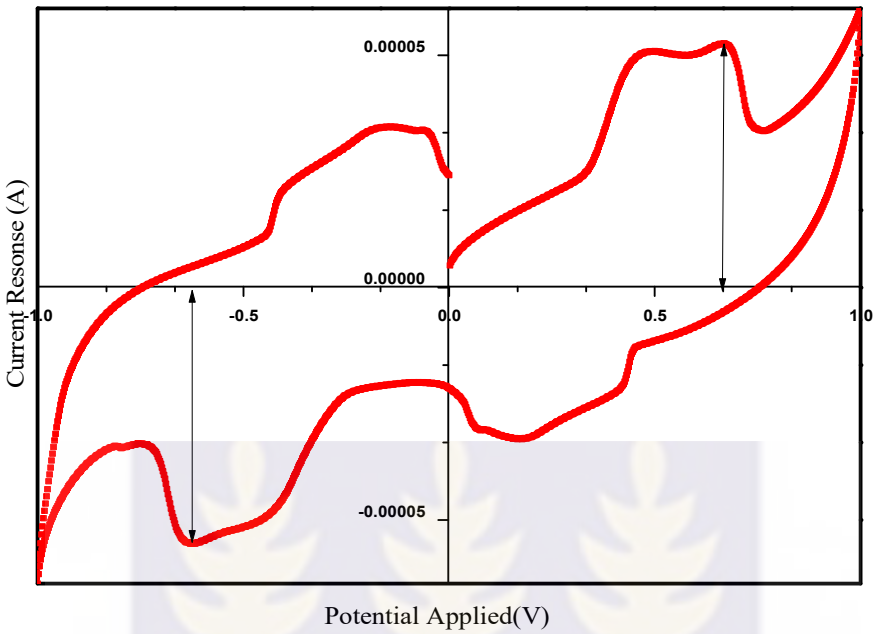

Figure 20: (c) Cyclic voltammogram of 1.0 mM urea.

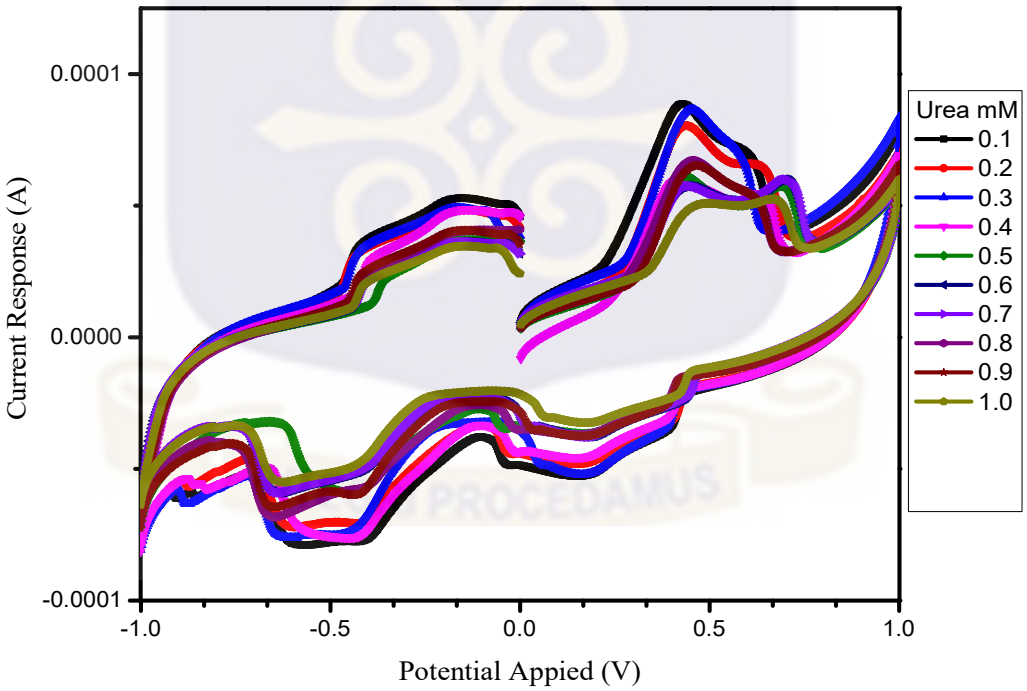

Figure 20: (d) Cyclic voltammogram of 0.1-1.0 mM urea superimposed for Zeolite X (Na) 70 °C modified biosensor.

4.2.4 Cyclic voltammogram of bioelectrode with Zeolite X (Na) 80 °C in selected urea concentrations

The peak anodic current which is proportional to the concentration of urea that is hydrolyzed by the urease enzyme on the bioelectrode surface with Zeolite X (Na) 80 °C for selected urea concentrations of 0.1 mM, 0.5 and 1.0 mM are as shown in figure 21 a-c respectively. All the 10 concentrations (0.1 mM – 1.0 mM) of urea for the same zeolite are depicted in figure 21 d, with the various determined anodic currents tabulated in table 3.

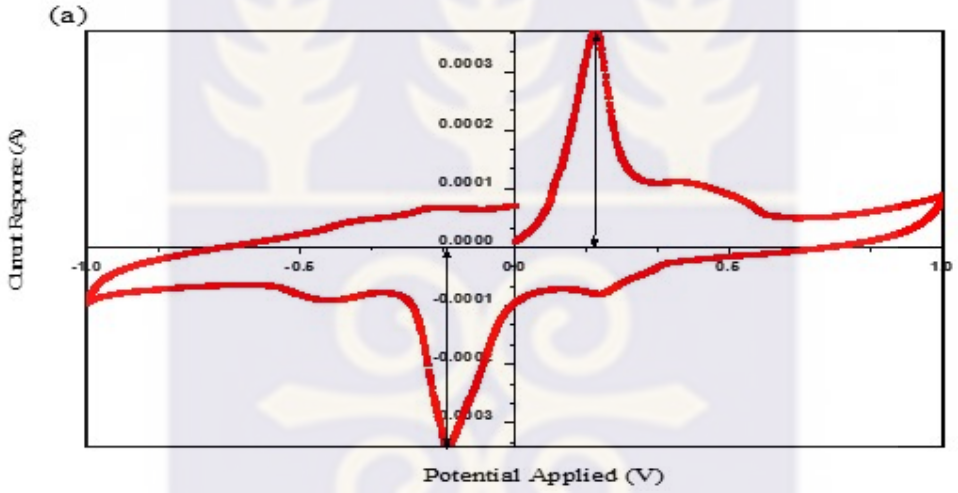

Figure 21: (a) Cyclic voltammogram of 0.1 mM urea

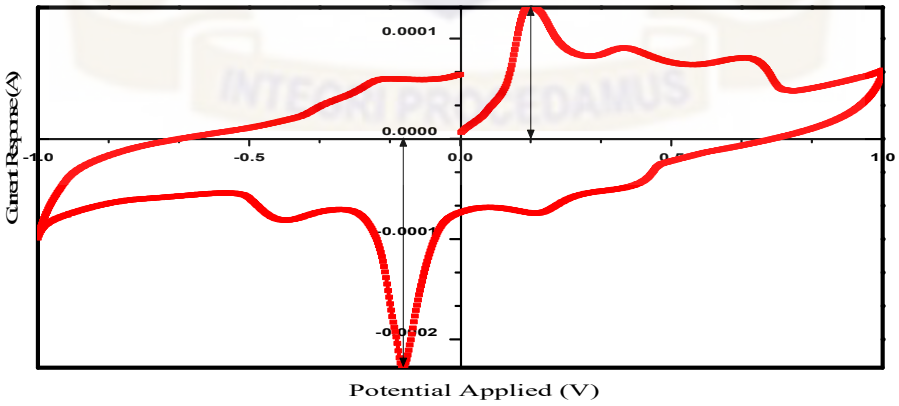

Figure 21: (b) Cyclic voltammogram of 0.5 mM urea.

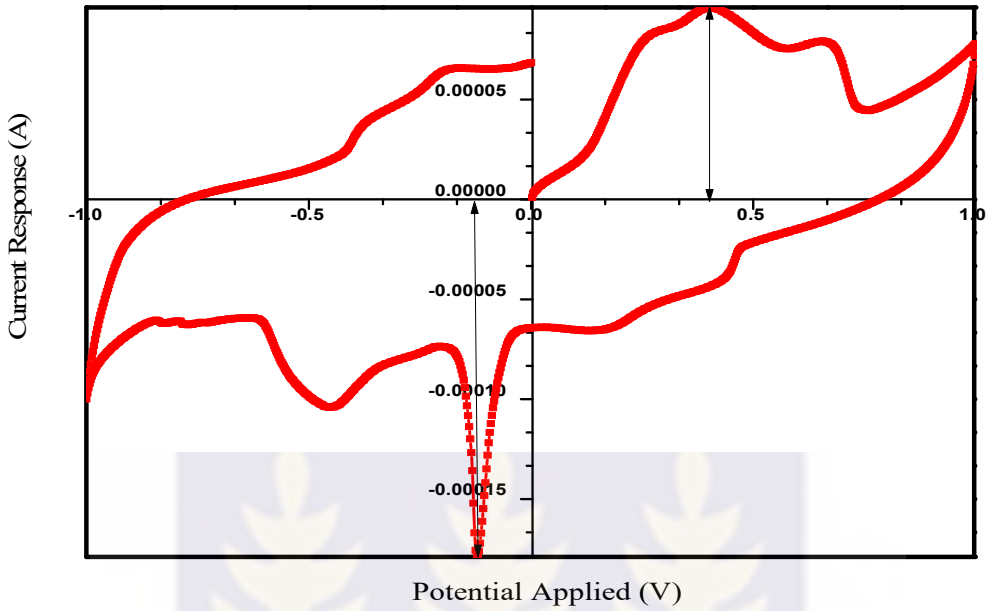

Figure 21: (c) Cyclic voltammogram of 1.0 mM urea.

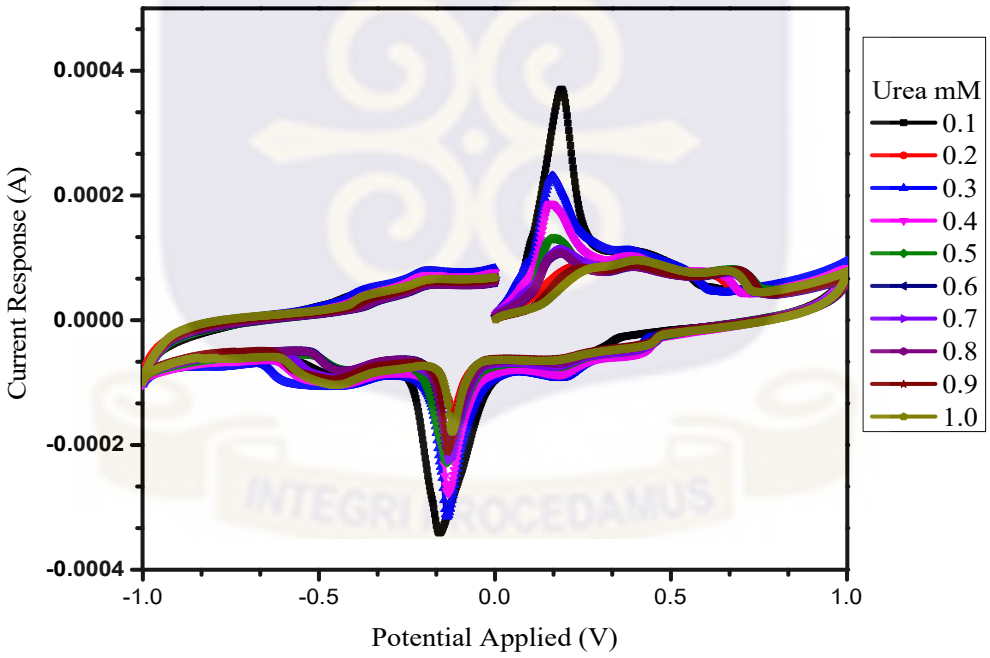

Figure 21: (d) Cyclic voltammogram of 0.1-1.0 mM urea superimposed for Zeolite X (Na) 80 °C modified biosensor.

4.3.5 Cyclic voltammogram of bioelectrode with Zeolite X (Na) 90 °C in selected urea concentrations.

The peak anodic current which is proportional to the concentration of urea that is hydrolyzed by the urease enzyme on the bioelectrode surface with Zeolite X (Na) 90 °C for selected urea concentrations of 0.1 mM, 0.5 and 1.0 mM are as shown in figure 22 a-c respectively. All the 10 concentrations (0.1 mM – 1.0 mM) of urea for the same zeolite are depicted in figure 22 d, with the various determined anodic currents tabulated in table 3.

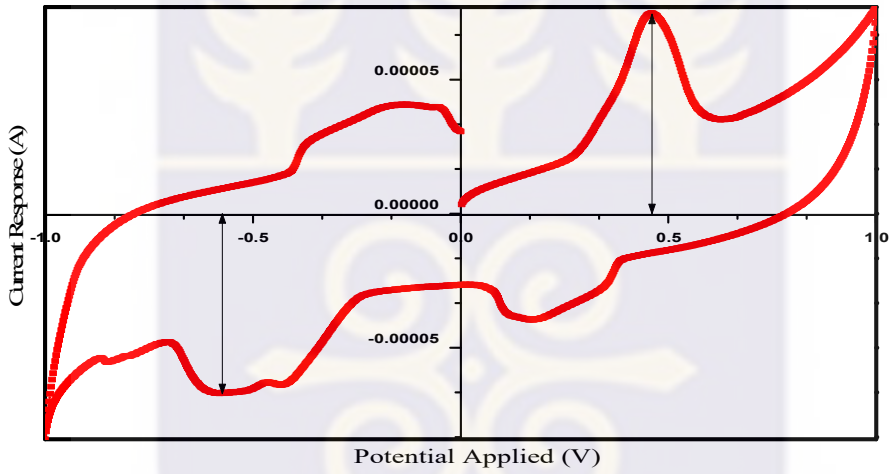

Figure 22: (a) Cyclic voltammogram of 0.1 mM urea.

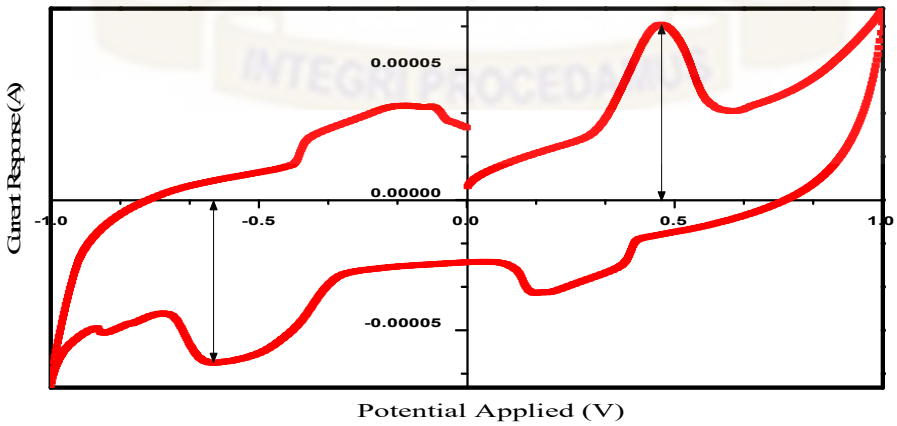

Figure 22: (b) Cyclic voltammogram of 0.5 mM urea.

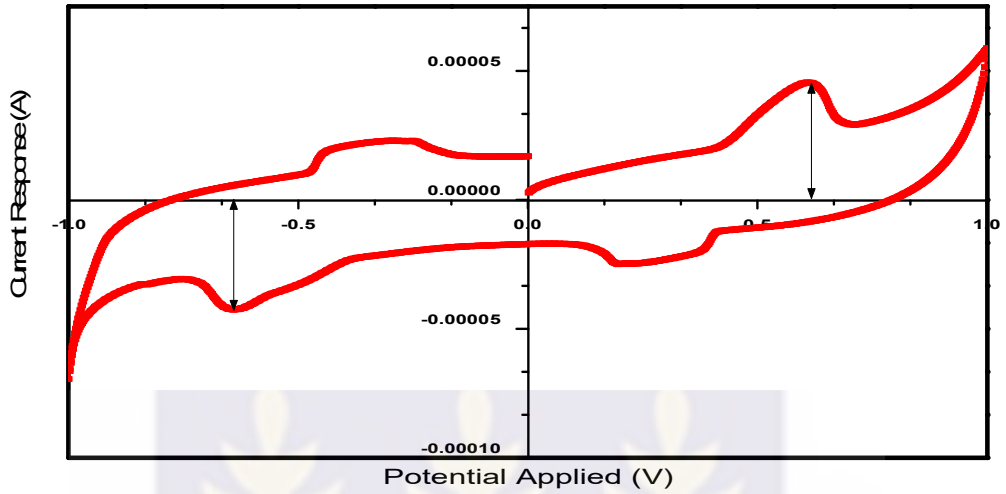

Figure 22: (c) Cyclic voltammogram of 1.0 mM urea.

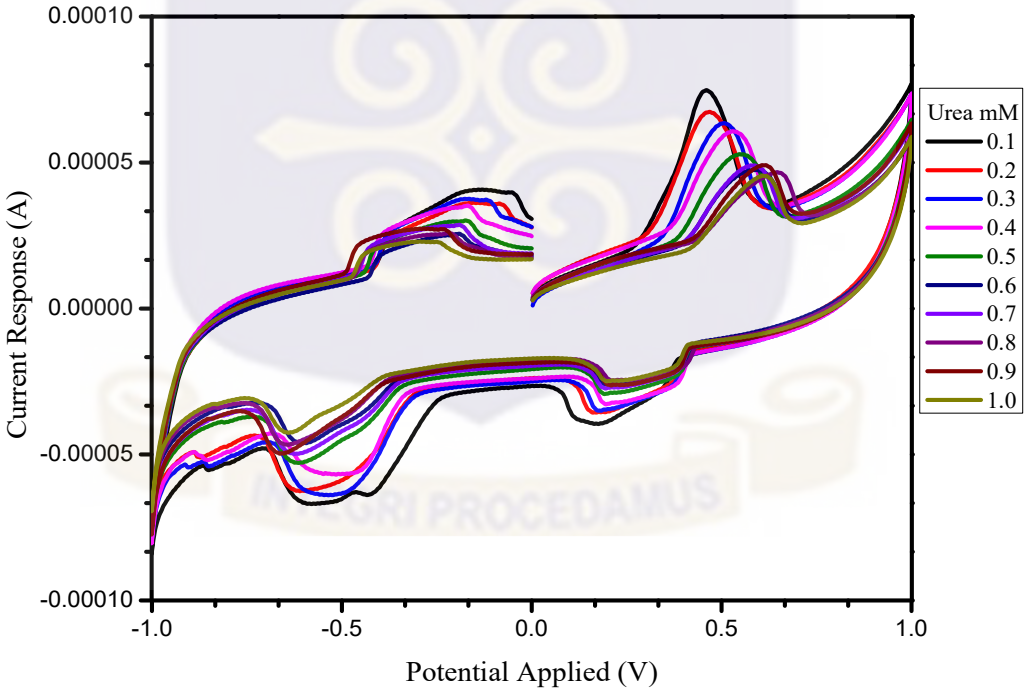

Figure 22: (d) Cyclic voltammogram of 0.1-1.0 mM urea superimposed for Zeolite X (Na) 90 °C modified biosensor.

4.3.6 Cyclic voltammogram of bioelectrode with Zeolite X (Na) 100 °C in selected urea concentrations.

The peak anodic current which is proportional to the concentration of urea that is hydrolyzed by the urease enzyme on the bioelectrode surface with Zeolite X (Na) 100 °C for selected urea concentrations of 0.1 mM, 0.5 and 1.0 mM are as shown in figure 23 a-c respectively. All the 10 concentrations (0.1 mM – 1.0 mM) of urea for the same zeolite are depicted in figure 23 d, with the various determined anodic currents tabulated in table 3.

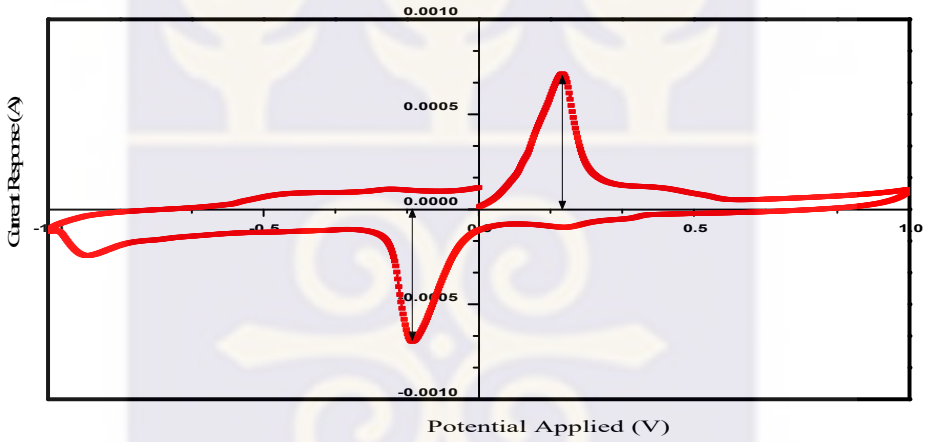

Figure 23: (a) Cyclic voltammogram of 0.1 mM urea.

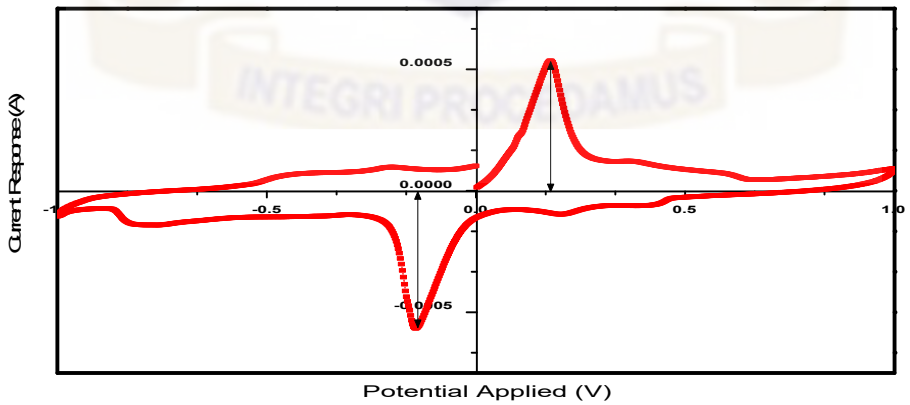

Figure 23: (b) Cyclic voltammogram of 0.5 mM urea.

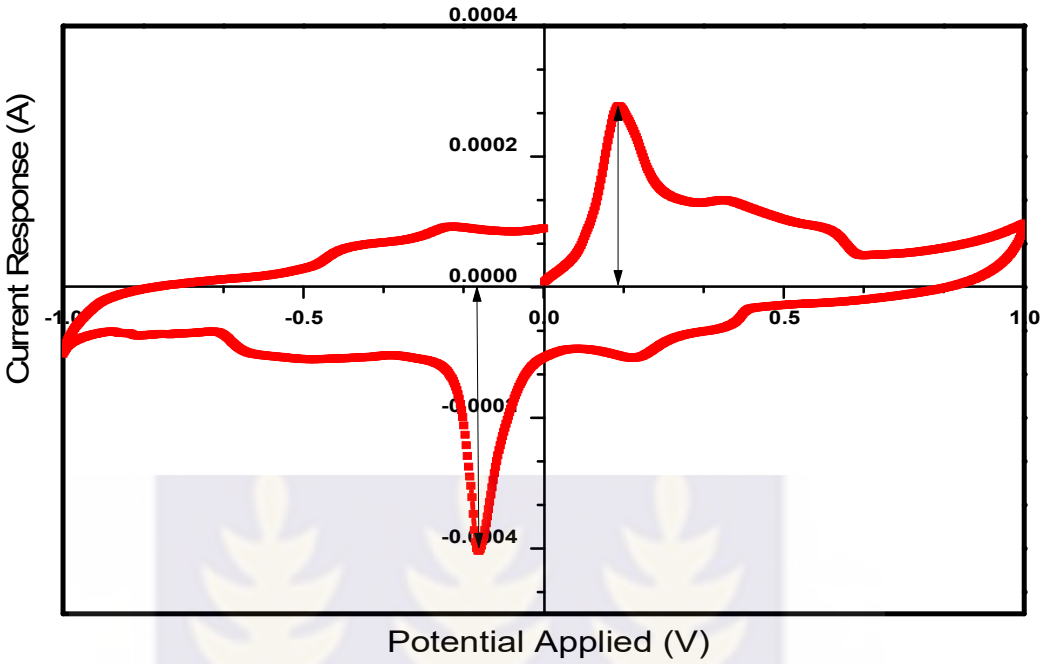

Figure 23: (c) Cyclic voltammogram of 1.0 mM urea.

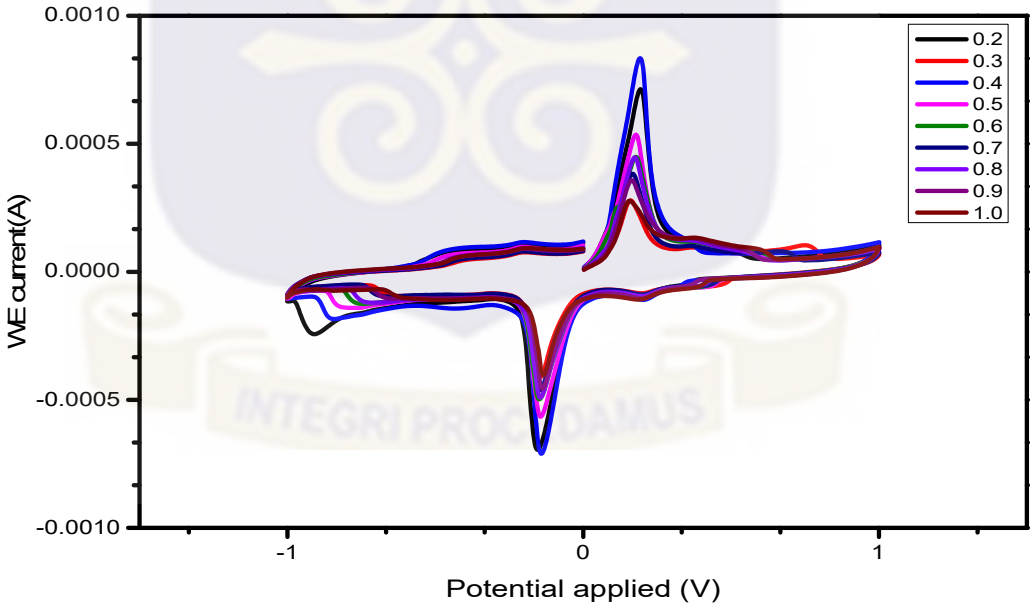

Figure 23: (d) Cyclic voltammogram of 0.1-1.0 mM urea superimposed Zeolite X (Na) for 100 °C modified biosensor.

4.4 Data Analysis

The peak anodic current was obtained from the various voltammograms; **Table 3** depicts urea recognition by enzyme-substrate interaction.

Table 3: Shows the peak anodic current for Zeolite X (Na) 60 °C - Zeolite X (Na) 100 °C obtained using EC-Lab® software.

Urea in mM	60°C	70°C	80°C	90°C	100°C
0.1	0.00010733	8.87146E-05	0.000370239	7.70874E-05	0.000834656
0.2	8.95386E-05	8.05054E-05	0.000231384	7.34863E-05	0.000724196
0.3	8.95386E-05	8.65479E-05	0.000187012	7.36084E-05	0.000713196
0.4	9.41467E-05	6.93054E-05	0.000130981	7.37305E-05	0.000535828
0.5	8.30994E-05	6.12793E-05	0.000113647	6.47278E-05	0.000449036
0.6	8.28552E-05	5.99945E-05	0.00010788	5.82855E-05	0.000446747
0.7	7.37915E-05	5.99945E-05	0.00010788	6.24695E-05	0.000383118
0.8	6.81763E-05	6.72302E-05	0.0001008	5.90942E-05	0.000357513
0.9	7.15942E-05	6.604E-05	9.61304E-05	6.3446E-05	0.000357513
1	6.80542E-05	6.00891E-05	8.82263E-05	5.88226E-05	0.000278595

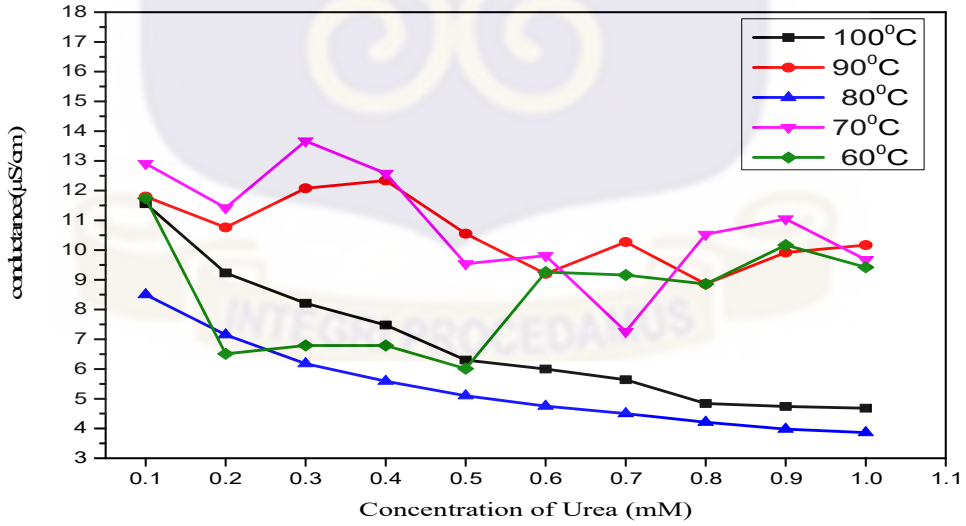

Figure 24: Molar conductance curve of Zeolite X (Na) modified electrodes and the response of the biosensor as a function of urea concentration.

On the basis of the linear detection range of 0.1-0.8 and 0.1-0.6 mM of the curves at Zeolite X (Na) 80 °C and Zeolite X (Na) 100 °C in figure 24 we conclude that crystallization temperature influences the conductance of Zeolite X (Na) 100 °C modified biosensors compared to Zeolite X (Na) 80 °C, but the regression coefficient prefers the former over the later.

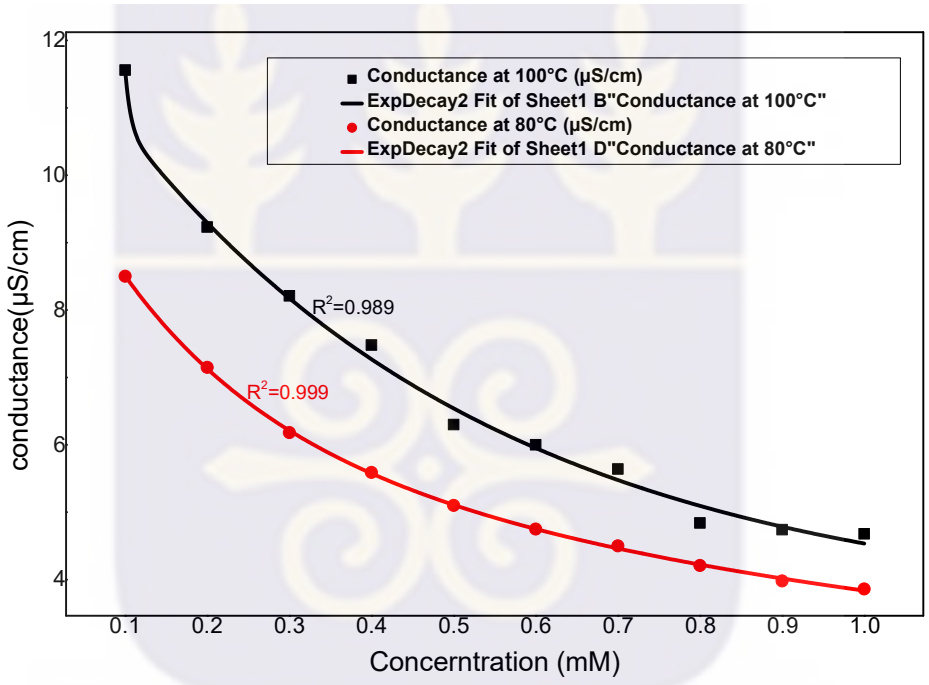

Figure 25: An exponential decay fit (type 2) of the conductance curve as a function of urea concentration by Zeolite X (Na) 100°C and Zeolite X (Na) 80°C respectively.

The exponential and fitted values are represented by the scatter plots and the solid lines respectively. The R-squared values computed is an indication of a highly steady decay profile of conductance measured with respect to urea concentration for both Zeolite X (Na) 100°C and Zeolite X (Na) 80°C.

CHAPTER FIVE

DISCUSSION

5.1 Discussion

The aim of this study was to investigate the effect of crystallization temperature on the kaolinite-based synthesis of zeolite and urease immobilization for potential fabrication of electrochemical urea biosensor. The synthesis of Zeolite X (Na) from kaolin was carried out as a function of the crystallization temperature, based on established methodologies from literature. The crystal phase identification of the individual materials was carried out by X-ray diffraction-methods and validated using a collection of simulated XRD powder patterns for zeolites. As shown in figure 16, the signature peaks labeled "K" and "Q" denote kaolinite and β-quartz peaks respectively, typical of kaolin XRD diffraction patterns. After calcining and undergoing fusion before hydrothermal (crystallization temperature) reaction from 60 °C to 100 °C, three kaolinite peaks at position 9, 12.5 and 25 completely disappeared, with new additional peaks formed as indicated by "x" (figure 16b–f). All of the peaks labeled "x" are confirmed signature peaks of Zeolite X (Na).

The peak intensities of Zeolite X (Na) were rather low, and this might be due to the formation of a small fraction of a crystalline phase sitting on an amorphous material. Nonetheless, all the crystallization temperatures produced Zeolite X (Na). The SEM results of Zeolite X (Na) indicate that there are significant amounts of the amorphous phase, which reflects the results obtained from the low-intensity XRD spectra. However, with regards to the morphological arrangement of particles, Zeolite X (Na) synthesized at 80 °C and 100 °C revealed well-defined crevices (figure 16c and 16e).

The Zeolite X (Na) 60 °C, Zeolite X (Na) 70 °C and Zeolite X (Na) 90 °C have comparable surface areas of 64, 68 and 113 m^2/g respectively, with an average pore size of 2 nm. The Zeolite X (Na) crystallised at 80 and 100 °C revealed a larger surface area, 295 and 389 m^2/g, respectively, with an average pore size of 4.5 nm, indicating that Zeolite X (Na) 80 °C and Zeolite X (Na) 100 °C can accommodate more urease. There is no clear explanation to the inconsistent behaviour of Zeolite X (Na) 90 °C with reference to the BET results obtained. These results are consistent with studies from poly (vinyl alcohol)-modified sol-gel materials, graphene, and gold nanoparticles, as well as zeolites for fabricating a urea biosensor, demonstrated by Doong's and other groups. The EDX data in Table 2 revealed that the Si/Al ratio is fairly constant, which is obvious because no additional source of Si and Al were introduced into the material. The estimation of crystallite size using Shearer's equation as well as other analytical tools also showed no significant differences in particle size as a function of the crystallization temperature and, therefore, the observed differences.

Cyclic voltammetry (CV) is an important and easy-to-use analytical tool to monitor charge transfer on an electrode surface through the electron transfer process. Urease was chosen due to its stability and has been widely applied in the fabrication of biosensors. The functioning of the urease biosensor is based on the reaction shown in Equation (1), in which the cleavage of urea into ammonium (NH_4^+) ions is as a result of proton consumption leading to charge transfer. Different methods for zeolite attachment to the transducer surface were used, and dip coating with baking at 200 °C turned out to be the most suitable method. The parameter-sets in Table 1 were used to measure CV signals as a result of the catalysis of the urea by the immobilized urease enzyme. The analytical control responses were measured as the cyclic voltammogram profiles for buffer only, buffer

and urease, buffer and urea, buffer, urease and 0.1 mM urea, and buffer, bio-zeolite and 0.1 mM urea as shown in figure 18. It was observed that the reaction rate of the bio-zeolite modified electrode was faster and enhanced compared to the urease on the surface of the gold electrode alone using the same amount of urea substrate. Again when we compared the cyclic voltammogram of the pure kaolin with Zeolite X (Na) 80 and 100 °C, there was a unique analytical response from the latter, indicating that the response was due to the synthesized zeolite rather than the amorphous phase. As a control, we compared the results with the free urease and found that the sensitivity of the immobilized enzyme was higher. It is important to note that the pure kaolin did not exhibit any analytical response.

As seen in figures 19d, 20d, 22d, there is a poor response of the biosensor at these crystallization temperatures, with the rate of response being erratic for Zeolite X (Na) synthesized at 60, 70 and 90 °C as compared Zeolite X (Na) 80 °C and Zeolite X (Na) 100 °C (figure 21d, 23d).

The Zeolite X (Na) material synthesized at 80 and 100 °C showed a better response than those synthesized at 60, 70 and 90 °C. This was further confirmed by the extremely high R-squared valued computed from the exponential decay fit model of their conductance curves. These peaks could be attributed to the oxidation and reduction of the enzymatically produced NH_4^+ ions. However, we cannot explain why there was no unique cyclic voltammogram of Zeolite X (Na) at 60, 70 and 90 °C even though the XRD spectra confirmed the formation Zeolite X (Na). It is, however, speculated that there must be well-

defined pore structures as in other two Zeolites for the effective immobilization of the substrate.

As shown in figure 24, the molar conductance of developed bio-zeolites at different crystallization temperatures was measured as a function of urea concentration (mM). The random response of the Zeolite X (Na) 60 °C, Zeolite X (Na) 70 °C, and Zeolite X (Na) 90 °C modified electrode with respect to urea concentration was attributed to the fact that the morphology of the material was not well defined; this resulted in the inefficient adsorption of the urease on the material as already speculated. The sensitivity of the urea biosensor at these temperatures was high but inconsequential due to the heterogeneous nature of the pore structures. An exponential regression analysis revealed R^2 values of 0.193, 0.299, 0.999, 0.350 and 0.989 for Zeolite X (Na) 60 °C, Zeolite X (Na) 70 °C, Zeolite X (Na) 80 °C, Zeolite X (Na) 90 °C and Zeolite X (Na) 100 °C respectively. In the case of Zeolite X (Na) 80 °C and Zeolite X (Na) 100 °C, there was a decay correlation due to the creation of a homogenous active surface area as a result of the formation of well-defined surface properties.

On the basis of the detection limit of 0.1– 0.8 and 0.1– 0.6 mM of the curves at 80 and 100 °C respectively as shown in figures 24, 25, we speculate that the material properties were influenced by parameters such as the crystallization temperature and pH variations. Even though the analytical response of Zeolite X (Na) 100°C showed high detection sensitivity as compared to Zeolite X (Na) 80°C, the decay analysis s the latter on the basis of the computed R^2 values. The cyclic voltammetry revealed oxidation and reduction peaks that indicate the successful immobilization of urease within the pore network in

Zeolite X (Na) 80 °C and Zeolite X (Na) 100 °C. To confirm this assertion, N_2 adsorption and desorption measurements were undertaken at 77 K and the results displayed in Table 2.

In this work, the only parameter that was adjusted was the crystallization temperature. Therefore, we precluded that this parameter was a critical determinant of the material properties which could influence enzyme immobilization. Certain temperatures would produce zeolites with good adsorbing characteristics with enhanced analytical responses, such as good detection limits and linearity in response, which had been key for developing good biosensors.

It is also worth noting that, all the experiments were conducted without electrolytic (charged electrolytes) additives; thus it is recommended for future studies that conductive electrolytes such as poly (3, 4-ethylene dioxythiophene), PEDOT, NaCl and KCl that could be used to modify the zeolites in order to optimize their conductance without the use of electrodes.

CHAPTER SIX

CONCLUSION AND RECOMMENTATION

6.1 CONCLUSION

In this study, we have demonstrated that zeolites synthesised from kaolin deposits in Ghana at different crystallization temperature can macromolecule immobilisation on the electrode surface. This has implication in the development of biosensors for various biomedical applications.

The findings in this study suggest that crystallization temperature influences the morphology of the zeolite, which consequently affects the adsorbed enzyme on the material surface. We did not perform our experiments with other commercial zeolites and also could not investigate the erratic behaviours of Zeolite X (Na) 60°C, Zeolite X (Na) 70°C as well as Zeolite X (Na) 90°C and suggest further studies in this regard. The test-of-concept approach is a promising endeavour to investigate further attributes of zeolites as immobilization agents and comparing with similarly produced commercially available zeolites.

6.2 RECOMMENDATION

We recommend that the response of the current zeolites be compared to their commercial available analogies. Further studies must also be conducted to determine the dynamic range of the detection. We also look forward to the advancement of producing screen printed kaolinite-base synthetic zeolite electrodes. The challenge with this work was that we could not estimate the amount of zeolite that is deposited on the surface of the gold

electrode, even though the same amount of zeolite paste was employed for the experiments that we carried out.

REFERENCES

[1] N Bhalla, P Jolly. N Formisan, P Estrela. Introduction to biosensors. Essays in biochemistry, 60 (2016), pp. 1-8.

[2] L. M. Muresan, Zeolite-modified electrodes with analytical applications. Pure Appl. Chem., 83 (2011), pp. 325–343.

[3] M. D. Gouda, M. A. Kumar, M. S. Thakur, N. G. Karanth, Enhancement of operational stability of an enzyme biosensor for glucose and sucrose using protein-based stabilizing agents, Biosens. Bioelectron. 17 (2002), pp. 503–507.

[4] D. Y. Kim, M. Kim, S. Shinde, J. S. Sung and G. Ghodake, Cytotoxicity and antibacterial assessment of gallic acid capped gold nanoparticles. Colloids and surfaces. B, Biointerfaces, 149 (2017), pp. 162-167.

[5] I. Kucherenko, O. Soldatkin, B. O. Kasap, S. K. Kirdeciler, B. A. Kurc, N. Jaffrezic-Renault, A. Soldatkin, F. Lagarde and S. Dzyadevych, Nanosized zeolites as a perspective material for conductometric biosensors. Nanoscale research letters, 10 (2015), pp. 209-218.

[6] S. Martin-Saldana, R. Palao-Suay, M. R. Aguilar, R. Ramirez-Camacho and J. San Roman, J. Polymeric nanoparticles loaded with dexamethasone or α-tocopheryl succinate to prevent cisplatin-induced ototoxicity. Acta Biomaterialia, 53 (2017), pp. 199–210.

[7] A. Bonanni and M. del Valle, Use of nanomaterials for impedimetric DNA sensors: A review. Analytica Chimica Acta, 678 (2010), pp. 7-17.

[8] D. J. Gorth, D. M. Rand and T. J. Webster, Silver nanoparticle toxicity in Drosophila: size does matter. International journal of nanomedicine, 6 (2011), pp. 343-350.

[9] N. Chauhan, S. Chawla, C. S. Pundir and U. Jain, an electrochemical sensor for detection of neurotransmitter-acetylcholine using metal nanoparticles, 2D material and conducting polymer modified electrode. Biosensors & Bioelectronics, 89 (Pt 1, 2017), pp. 377-383.

[10] B. Ozansoy Kasap, S. V. Marchenko, O. O. Soldatkin, S. V. Dzyadevych and B. Akata Kurc, Biosensors Based on Nano-Gold/Zeolite-Modified Ion-Selective Field-Effect Transistors for Creatinine Detection. Nanoscale research letters, 12 (2017), pp. 162.

[11] M. P. Prabhakaran, L. Ghasemi-Mobarakeh, G. Jin and S. Ramakrishna, Electrospun conducting polymer nanofibers and electrical stimulation of nerve stem cellsJournal of bioscience and bioengineering, 112 (2011), pp. 501-507.

[12] C. Shan, H. Yang, D. Han, Q. Zhang, A. Ivaska and L. Niu, Graphene/AuNPs/chitosan nanocomposites film for glucose biosensing. Biosensors & Bioelectronics, 25 (2010), pp. 1070-1074.

[13] D. G. Cabral, E. C. Lima, P. Moura and R. F. Dutra, A label-free electrochemical immunosensor for hepatitis B based on hyaluronic acid–carbon nanotube hybrid film Talanta, 148 (2016), pp. 209-215.

[14] C. Mousty, Biosensing applications of clay-modified electrodes: a review. Analytical and bioanalytical chemistry, 396 (2010), pp. 315-325.

[15] M. Chakraborti, J. K. Jackson, D. Plackett, D. M. Brunette and H. M. Burt, Drug intercalation in layered double hydroxide clay: Application in the development of a nanocomposite film for guided tissue regeneration. International journal of pharmaceutics, 416 (2011), pp. 305-313.

[16] M. Liu, R. He, J. Yang, W. Zhao and C. Zhou, Stripe-like Clay Nanotubes Patterns in Glass Capillary Tubes for Capture of Tumor Cells. ACS applied materials & interfaces, 8 (2016), pp. 7709-7719.

[17] A. S. Olatunji, J. O. Olajide-Kayode and A. F. Abimbola, Evaluation of geochemical characteristics and health effects of some geophagic clays southern Nigeria Environmental geochemistry and health, 36 (2014), pp. 1105-1114.

[18] D. L. Guerra, R. R. Viana and C. Airoldi, RETRACTED: Application of natural and modified hectorite clays as adsorbents to removal of Cr (VI) from aqueous solution–Thermodynamic and equilibrium study. Journal of hazardous materials, 172 (2009), pp. 507-514.

[19] Y. Jin, N. Zhang, C. Li, K. Pu, C. Ding and Y. Zhu, Nanosystem composed with MSNs, gadolinium, liposome and cytotoxic peptides for tumor theranostics. Colloids and surfaces. B, Biointerfaces, 151(2017), pp. 240-248

[20] J. K. Oh, C. Tang, H. Gao, N. V. Tsarevsky and K. Matyjaszewski, Inverse Miniemulsion ATRP: A New Method for Synthesis and Functionalization of Well-Defined Water-Soluble/Cross-Linked Polymeric Particles. Journal of the American Chemical Society, 128 (2006), pp. 5578-5584.

[21] H. Sangodkar, S. Sukeerthi, R. S. Srinivasa, R. Lal and A. Q. Contractor, A Biosensor Array Based on Polyaniline. Analytical Chemistry, 68 (1996), pp. 779-783.

[22] L. T. Nguyen and H. H. Yoon, Potentiometric Urea Biosensor Based on Carbon Nanotubes and Polyion Complex Film. Journal of nanoscience and nanotechnology, 15 (2015), pp. 1150-1153.

[23] Z. A. Ansari, S. G. Ansari, H. K. Seo, Y. S. Kim and H. S. Shin, Urea Sensing Characteristics of Titanate Nanotubes Deposited by Electrophoretic Deposition Method. Journal of nanoscience and nanotechnology, 11 (2011), pp. 3323-3329.

[24] D. Liu, K. Chen, K. Ge, L. Nie and S. Yao, A new urea sensor based on combining the surface acoustic wave device with urease extracted from green soya bean and its application— determination of urea in human urine. Biosensors & Bioelectronics, 11 (1996), pp. 435-442.

[25] J. Shalini, K. J. Sankaran, C. Y. Lee, N. H. Tai and I. N. Lin, An amperometric urea biosensor based on covalent immobilization of urease on N_2 incorporated diamond nanowire electrode. Biosensors & Bioelectronics, 56 (2014), pp. 64-70.

[26] V. N. Pyeshkove, O. Y Dudchenko, O. O. Soldatkin, I. Kucherenko, B.O. Kasap,B.A. Kurc, S V. Dzyandey "Application of silicalite for improvement of enzyme adsorption on the stainless steel electrodes," Biopolymers and cell, 30 (2013), pp. 462-468.

[27] Mao, X., Baloda, M., Gurung, A. S., Lin, Y., & Liu, G.. Multiplex electrochemical immunoassay using gold nanoparticle probes and immunochromatographic strips. Electrochemistry Communications, 10 (2008), pp. 1636–1640.

[28] Y. Zhengpeng, S. Shihui, D. Hongjuan, Z. Chunjing, Piezoelectric urea biosensor based on immobilization of urease onto nanoporous alumina membranes Biosensors and Bioelectronics, 22 (2007), pp. 3283-3287.

[29] Zhang, G. J., & Ning, Y. Silicon nanowire biosensor and its applications in disease diagnostics: A review Analytica Chimica Acta., 749 (2012), pp. 1-15.

[30] T. Osaka, S. Komaba, M. Seyama, K. Tanabe, High-sensitivity urea sensor based on the composite film of electro-inactive polypyrrole with polyion complex, Sens. Actuators B Chem., 36 (1996), pp. 463–469.

[31] M. Gutierrez, S. Alegret, M. Valle, Potentiometric bioelectronic tongue for the analysis of urea and alkaline ions in clinical samples, Biosens. Bioelectron., 22 (2007), pp. 2171–2178

[32] M. Gronow, Biosensors, Trends Biochem. Sci., 9 (1984), pp. 336–340.

[33] M. Singh, N. Verma, A. K. Garg, and N. Redhu. Urea biosensors. Sensors and Actuators B : Chemical, 134 (2008), pp. 345–351.

[34] Z. Junhui, C. Hong, and Y. Ruifu, "DNA based biosensors," biotechnology advances, 15 (1997), pp. 43–58.

[35] J. F. Cassidy, A. P. Doherty, J. G. Vos, in Principles of Chemical and Biological Sensors. (Ed: D. Diamond), Wiley, Toronto 1998.

[36] S. Cosnier," Biosensors based on electro-polymerized films: new trends" Anal. Bioanal. Chem., 377 (2003), pp. 507-520.

[37] W. H. Scouten, J. H. T. Luong, and R. S. Brown, "Enzyme or protein immobilization techniques for applications in biosensor design," Reviews, 13 (1995), pp. 178-185.

[38] J.F. Kennedy, J.M.S. Cabral, in H.J. Rehm, G. Reed (Eds.), Biotechnology, 7a, VCH Publishers, Germany, 1987, pp. 349–404.

[39] J.H.T. Luong, A. Mulchandani, G.G. Guilbault, Developments and applications of biosensors, Trends Biotechnol., 6 (1988), pp. 310–316.

[40] N. Tinkilic, O. Cubuk, I. Isildak, 'Glucose and urea biosensors based on all solid-state PVC–NH2 membrane electrodes'Anal. Chim. Acta., 452 (2002), pp. 29-34.

[41] M.L. Hamlaoui, K. Reybier, M. Marrakchi, N. Jaffrezic-Renault, C. Martelet, R. Kherrat, A. Walcarius, 'Development of a urea biosensor based on a polymeric membrane including zeolite'Anal. Chim. Acta., 466 (2002), pp. 39–45.

[42] A. Sassolas, L.S Blum and B.D, Leca-Bovier. Immobilization strategies to develop enzymatic biosensors, Biotechnology Advances, 30 (2012), pp. 489-571.

[43] S.K. Sharma, R. Singhal, B.D. Malhotra, N. Sehgal, A. Kumar Langmuir–Blodgett film based biosensor for estimation of galactose in milk**.** Electrochim Acta, 49 (2004), pp. 2479–2485.

[44] Kimmel DW, LeBlanc G, Meschievitz ME, Cliffel DE. Electrochemical sensors and biosensors. Anal Chem., 84 (2012), pp.685–707.

[45] Teles FRR, Fonseca LP. Applications of polymers for biomolecule immobilization in electrochemical biosensors. Mater Sci Eng C, 28 (2008), pp.1530–1543.

[46] M. Campas, B. Bucur, S. Andreescu, J.-L. Marty Application of oriented immobilisation to enzyme sensors, Curr Top Biotechnol., 1 (2004), pp. 95–107.

[47] C. Bonnet, S. Andreescu, J.L. Marty Adsorption: an easy and efficient immobilisation of acetylcholinesterase on screen-printed electrodes, Anal Chim Acta, 481 (2003), pp. 209–211.

[48] S. Andreescu, L. Barthelmebs, J.L. Marty Immobilization of acetylcholinesterase on screen-printed electrodes: a comparative study between three immobilization methods and applications to the detection of organophosphorus insecticides, Anal Chim Acta, 464 (2002), pp. 171–180.

[49] E.V. Gogol, G.A. Evtugyn, J.L. Marty, H.C. Budnikov, V.G. Winter Amperometric biosensors based on nafion coated screen-printed electrodes for the determination of cholinesterase inhibitors, Talanta, 53 (2000), pp. 379–389.

[50] J. Zhang, D. Shan, S.L. Mu. Improvement in selectivity and storage stability of a choline biosensor fabricated from poly(aniline-co-o-aminophenol), Front Biosci., 12 (2007), pp. 783–790.

[51] Z. Zhang, S. Xia, D. Leonard, N. Jaffrezic-Renault, J. Zhang, F. Bessueille, A novel nitrite biosensor based on conductometric electrode modified with cytochrome reductase composite membrane Biosensor Bioelectron, 24 (2009), pp. 1574–1579.

[52] N. Bruns, J.C. Tiller Amphiphilic networks as nanoreactor for enzymes on organic solvents Nano Lett., 5 (2005), pp. 45–48.

[53] M. Hanko, N. Bruns, J.C. Tiller, J. Heinze Optical biochemical sensor for determining hydroperoxides in nonpolar organic liquids as archetype for sensors consisting of amphiphilic networks as immobilisation matrices. Anal Bioanal Chem., 386 (2006), pp. 1273–1283.

[54] M.M.F. Choi Progress in enzyme-based biosensors using optical transducers, Microchim Acta, 148 (2004), pp. 107–132.

[55] L. Cao. Immobilised enzymes: science or art, Curr Opin Chem Biol., 9 (2005), pp. 217–226.

[56] J.M. Guisan Methods in biotechnology: immobilization of enzymes and cells,

(Second edition) Humana Press Totowa, New Jersey (2006)

[57] G.T. Hermanson Bioconjugate techniques), Academic Press, San Diego (2008)

[58] B.D. Leca, L.J. Blum Luminol electrochemiluminescence with screen-printed electrodes for low-cost disposable oxidase-based optical sensors Analyst, 125 (2000), pp. 789–791

[59] K.R. Rogers Recent advances in biosensor techniques for environmental monitoring, Anal Chim Acta, 568 (2006), pp. 222–231.

[60] S. Datta, L. R. Christena, Y. R. S. Rajaram. Enzyme immobilization: an overview on techniques and support materials. Biotechnology, 3 (2013) pp.1-9.

[61] S. Zhang *, G. Wright, Y. Yang. Materials and techniques for electrochemical biosensor design and construction. Biosensors and Bioelectronics, 15 (2000), pp. 273-282.

[62] M.D. Gouda, M.A. Kumar, M.S. Thakur, N.G. Karanth, Enhancement of operational stability of an enzyme biosensor for glucose and sucrose using protein-based stabilizing agents, Biosens. Bioelectron. 17 (2002), pp. 503–507.

[63] Salih Kaan Kirdeciler a, Esin Soya, Sec¸ kin Ozturka, c, Ivan Kucherenkob, Oleksandr Soldatkinb, Sergei Dzyadevychb, d, Burcu Akataa, c, A novel urea conductometric biosensor based on zeolite immobilized urease. 85 (2011), pp. 1435-1441.

[64] C. Senaratne. J. Zhuang, J. Fox, I. Burgess, M. D. Baker, 'Electroanalytical chemistry with zeolites', Microporous and mesoporous Mater., 403 (1999), pp.281-289.

[65] A. Walcarius, P. Mariaulle, L. Lamberts, 'Use of a zeolite-modified electrode for the study of the methyl viologen-sodium ion-exchange in zeolite Y, J. Electroanalytical Chem., 463 (1999), pp. 100-108.

[66] Rios C. A., William C. D., M. M. J. Synthesis of Zeolites and Zeotypes by Hydrothermal Transformation of Kaolinite and Metakaolinite. Bistua, 5(2007), pp.15–26.

[67] Tiburu, E. K.; Fleischer, H. N. a.; Aidoo, E. O.; Salifu, A. a.; Asimeng, B. O.; Zhou, H. Crystallization of Linde Type A Nanomaterials at Two Temperatures Exhibit Differential Inhibition of HeLa Cervical Cancer Cells In Vitro; J. Biomimetics, Biomater. Biomed. Eng., 28 (2016), pp. 66–77.

[68] Ríos, C. A.; Williams, C. D.; Fullen, M. A. Nucleation and growth history of zeolite LTA synthesized from kaolinite by two different methods. Appl. Clay Sci., 42 (2009), pp. 446–454.

[69] Alkan, M.; Hopa, Ç.; Yilmaz, Z.; Güler, H. The effect of alkali concentration and solid/liquid ratio on the hydrothermal synthesis of zeolite NaA from natural kaolinite. Microporous Mesoporous Mater., 86 (2005), pp. 176–184.

[70] Murayama, N.; Yamamoto, H.; Shibata, J. Mechanism of zeolite synthesis from coal fly ash by alkali hydrothermal reaction. Int. J. Miner. Process. 64 (2002), pp. 1–17.

[71] Ojha, K.; Pradhan, N. C.; Samanta, A. N. Zeolite from fly ash: Synthesis and characterization. Bull. Mater. Sci., 27 (2004), pp. 555-564.

[72] Querol, X.; Moreno, N.; Umaa, J. C.; Alastuey, A.; Hernández, E.; López-Soler, A.; Plana, F. Synthesis of zeolites from coal fly ash: an overview. Int. J. Coal Geol., 50 (2002), pp. 413-423

[73] Inada, M.; Eguchi, Y.; Enomoto, N.; Hojo, J. Synthesis of zeolite from coal fly ashes with different silica-alumina composition. Fuel. 84 (2005), pp. 299-304.

[74] Hollman, G. G.; Steenbruggen, G.; Janssen-Jurkovičová, M. A two-step process for the synthesis of zeolites from coal fly ash. Fuel. 78 (1999), pp. 1225-1230.

[75]. Chareonpanich, M.; Namto, T.; Kongkachuichay, P.; Limtrakul, J. Synthesis of ZSM-5 zeolite from lignite fly ash and rice husk ash. Fuel Process. Technol., 85 (2004), pp. 1623-1634.

[76] Mohamed, M. M.; Zidan, F. I.; Thabet, M. Synthesis of ZSM-5 zeolite from rice husk ash: Characterization and implications for photocatalytic degradation catalysts. Microporous Mesoporous Mater., 108 (2008), pp. 193-203.

[77] Kordatos, K.; Gavela, S.; Ntziouni, A.; Pistiolas, K. N.; Kyritsi, A.; Kasselouri-Rigopoulou, V. Synthesis of highly siliceous ZSM-5 zeolite using silica from rice husk ash. Microporous Mesoporous Mater., 115 (2008), pp. 189-196.

[78] Dorothee Grieshaber, Robert MacKenzie, Janos Voros and Erik Reimhult. Electrochemical Biosensors - Sensor Principles and Architectures. Sensors, 8 (2008), pp. 1400-1458.

[79] Ce´spedes, F., Alegret, S. New materials for electrochemical sensing: glucose biosensors based on rigid carbon-polymer biocomposites. Food Technol. Biotechnol., 34 (1996), pp. 143–146.

[80] O. O. Soldatkin, I. S. Kucherenko S. V. Marchenko, B. O. Kasap, B. Akata, and A. P. Soldatkin, S. V. Dzyadevych, "Application of enzyme/zeolite sensor for urea analysis in serum," Mater. Sci. Eng. C, 42 (2014), pp.155-160 .

[81] M. Gerard, A. Chaubey, and B. D. Malhotra, "Application of conducting polymers to biosensors," biosensors and bioelectronics, 17 (2002), pp. 345–359.

[82] C. Belviso, F. Cavalcante, A. Lettino, S. Fiore. A and X-type zeolites synthesised from Kaolinite at low temperature, Applied Clay Science, 80–81 (2013), pp. 162–168.

APPENDIX A

Cyclic Voltammogram of Base Material Kaolin

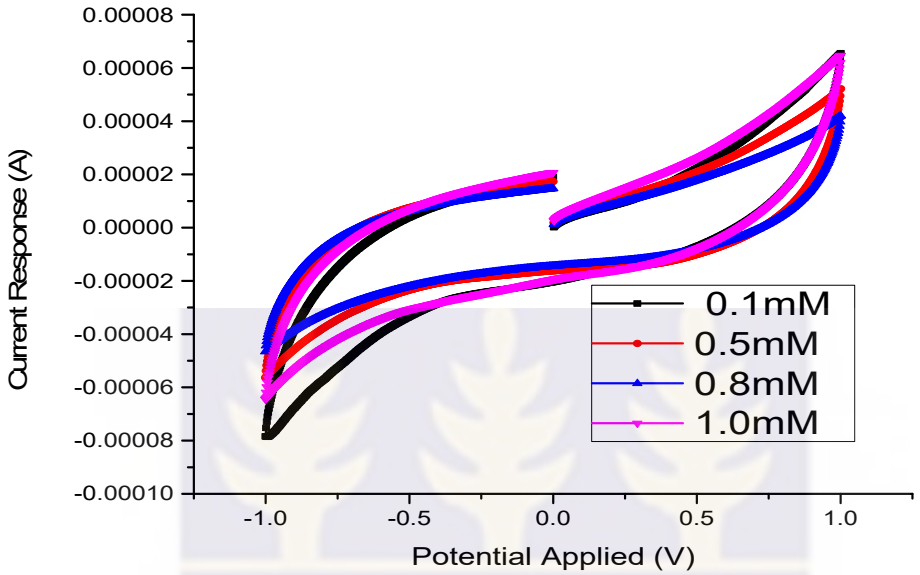

Figure 26: Cyclic Voltammogram of Kaolinite with selected Concentrations (0.1, 0.5, 0.8, 1.0 mM) of Urea

There is no observed anodic and cathodic peak with the voltammogram from the base material Kaolinite. The observed peaks are as a result of the set parameters for the cyclic voltammetry as indicated in **Table 1**.

APPENDIX B

Exponential Fitting Data Generated by Origin Pro 9 Software for Conductance of Zeolite X (Na) 60 °C.

Parameters

		Value	Standard Error
Conductance at 60 °C	Intercept	10.601	1.96989
	B1	-13.34924	8.22709
	B2	13.53788	7.28889

Statistics

	Conductance at 60 °C
Number of Points	10
Degrees of Freedom	7
Residual Sum of Squares	19.63608
Adj. R-Square	0.19278

Summary

	Intercept		B1		B2		Statistics
	Value	Standard Error	Value	Standard Error	Value	Standard Error	Adj. R-Square
Conductance at 60 °C	10.601	1.96989	-13.34924	8.22709	13.53788	7.28889	0.19278

Anova

		DF	Sum of Squares	Mean Square	F Value	Prob>F
Conductance at 60 °C	Model	2	11.63961	5.81981	2.07468	0.1961
	Error	7	19.63608	2.80515		
	Total	9	31.27569			

APPENDIX C

Exponential Fitting Data Generated by Origin Pro 9 Software for Conductance of Zeolite X (Na) 70 °C.

Parameters

		Value	Standard Error
Conductance of Zeolite X (Na) 70 °C	Intercept	14.56	1.87684
	B1	-11.88788	7.83847
	B2	7.33333	6.94459

Statistics

	Conductance at 70 °C
Number of Points	10
Degrees of Freedom	7
Residual Sum of Squares	17.82481
Adj. R-Square	0.29938

Summary

	Intercept		B1		B2		Statistics
	Value	Standard Error	Value	Standard Error	Value	Standard Error	Adj. R-Square
Conductance at 70 °C	14.56	1.87684	-11.8878	7.83847	7.33333	6.94459	0.29938

Anova

		DF	Sum of Squares	Mean Square	F Value	Prob>F
Conductance at 70 °C	Model	2	14.88584	7.44292	2.92292	0.11945
	Error	7	17.82481	2.5464		
	Total	9	32.71065			

APPENDIX D

Exponential Fitting Data Generated by Origin Pro 9 Software for Conductance of Zeolite X (Na) 80 °C.

Parameters

		Value	Standard Error
Conductance at 80 °C	Intercept	9.326	0.22205
	B1	-11.50879	0.92739
	B2	6.19697	0.82163

Statistics

	Conductance at 80 °C
Number of Points	10
Degrees of Freedom	7
Residual Sum of Squares	0.24951
Adj. R-Square	0.98431

Summary

	Intercept		B1		B2		Statistics
	Value	Standard Error	Value	Standard Error	Value	Standard Error	Adj. R-Square
Conductance at 80 °C	9.326	0.22205	-11.50879	0.92739	6.19697	0.82163	0.98431

Anova

Conductance at 80 °C		DF	Sum of Squares	Mean Square	F Value	Prob>F
	Model	2	20.19085	10.09542	283.22668	2.00955E-7
	Error	7	0.24951	0.03564		
	Total	9	20.44036			

APPENDIX E

Exponential Fitting Data Generated by Origin Pro 9 Software for Conductance of Zeolite X (Na) 90 °C.

Parameters

		Value	Standard Error
Conductance at 90 °C	Intercept	12.5195	1.11448
	B1	-4.93356	4.65453
	B2	2.04924	4.12374

Statistics

	Conductance at 90 °C
Number of Points	10
Degrees of Freedom	7
Residual Sum of Squares	6.28512
Adj. R-Square	0.34987

Summary

Con-ductance at 90 °C	Intercept		B1	B2	Statistics		
	Value	Stand-ard Er-ror	Value	Standard Error	Value	Stand-ard Er-ror	Adj. R-Square
	12.5195	1.11448	-4.93356	4.65453	2.04924	4.12374	0.34987

Anova

Conduct-ance at 90 °C		DF	Sum of Squares	Mean Square	F Value	Prob>F
	Model	2	6.14453	3.07226	3.42171	0.09194
	Error	7	6.28512	0.89787		
	Total	9	12.42965			

APPENDIX F

Exponential Fitting Data Generated by Origin Pro 9 Software for Conductance of Zeolite X (Na) 100 °C.

Parameters

		Value	Standard Error
Conductance at 100 °C	Intercept	12.71617	0.37504
	B1	-16.93568	1.56632
	B2	9.00379	1.3877

Statistics

	Conductance at 100 °C
Number of Points	10
Degrees of Freedom	7
Residual Sum of Squares	0.71174
Adj. R-Square	0.98001

Summary

	Intercept		B1		B2		Statistics
	Value	Stand-ard Er-ror	Value	Stand-ard Er-ror	Value	Stand-ard Error	Adj. R-Square
Con-duct-ance at 100 °C	12.71617	0.37504	-16.9356	1.56632	9.00379	1.3877	0.98001

Anova

Conductance at 100 °C		DF	Sum of Squares	Mean Square	F Value	Prob>F
	Model	2	45.07022	22.53511	221.63403	4.68483E-7
	Error	7	0.71174	0.10168		
	Total	9	45.78196			

APPENDIX G

PLAGIARISM REPORT

Turnitin Originality Report

Processed on: 19-Jul-2017 15:33 GMT

ID: 831822523

Word count: 12331

Plagiarism check for **"INVESTIGATING THE INFLUENCE OF TEMPERATURE ON KAOLINITE-BASE SYNTHESIS OF ZEOLITE AND UREASE IMMOBILIZATION FOR POTENTIAL FABRICATION OF ELECTROCHEMICAL UREA BIOSENSOR"** by Anderson Ebo David

Similarity index: 13%

Similarity by source

Internet source: 7%

Publications: 10%

Student Papers: 2%